Mixed Valency Chemistry: A Survey of 10 Years Progress

Peter Day[a]

[a] Inorganic Chemistry Laboratory, Oxford University, Oxford, UK

PLEASE SCROLL DOWN FOR ARTICLE

MIXED VALENCY CHEMISTRY:
A SURVEY OF 10 YEARS PROGRESS

PETER DAY

*Inorganic Chemistry Laboratory, Oxford University,
South Parks Road, Oxford OX1 3QR, UK*

INTRODUCTION: HISTORICAL BACKGROUND

Mixed valency chemistry is literally as old as the hills. Minerals such as vivianite, crocidolite, voltaite and above all magnetite testify to the existence of lattices containing an element (in this case Fe) in two different oxidation states on the geological time scale. Only slightly more recently primitive microorganisms began to see the evolutionary advantages of employing mixed valency clusters of Fe bound to S as oxidation-reduction enzymes, no doubt because the small atom rearrangements which accompany the change in oxidation state, further described below, mean that the activation energy of the process is suitably low. In historical times mixed valency came into technology via dyestuffs such as Prussian Blue (17th–18th century). The latter half of the 19th century saw preparative inorganic chemists like Alfred Werner (1896) taking a strong interest in the phenomenon, for example in his pioneering work on the bis-oxalatoplatinites which we now know as among the first linear-chain molecular metals. Indeed, it was he who recognized the analogy between these compounds and the tungsten bronzes, prepared some 20 years earlier by Biltz.

Qualitative theories connecting colour with chemical constitution, and giving prominence to charge transfer from one ion to another in mixed oxidation state compounds, were common in the first 20 years of the present century (e.g. Hofmann and Hoschele, 1916). Starting in the 1930s, and continuing after the Second World War, solid state physicists like Verwey at the Philips Laboratory, Eindhoven, uncovered the connections between conductivity and mixed valency in oxides such as $Li_xNi_{1-x}O$ and $La_{1-x}SrMnO_3$, known as 'controlled valency semiconductors' (e.g. Verwey *et al.*, 1950). At the same time, in a parallel development, came work on the oxidation-reduction mechanisms of metal complexes in solution which drew attention to mixed valency oligomers as potentially tractable models for studying redox phenomena. Still, in spite of the long history of mixed valency in chemistry just described, there appeared to be no general realization by physical inorganic chemists that mixed valency compounds might have interesting and rewarding properties as a class, rather than haphazardly encountered individual examples. In 1967 two reviews (Robin and Day, 1967; Allen and Hush, 1967) appeared which aimed to remedy this situation, in the event, it can now be seen, successfully. Of the two accounts published in 1967 that by Hush related mixed valency phenomena to theories of inner- and outer-sphere electron transfer in solution while that of Robin and the present author collected a large body of examples from all over the Periodic Table, and showed how their physical properties could be related to molecular and crystal structures in terms of the degree of similarity, or difference, between the coordination sites occupied by the ions of different oxidation states.

During the last 10 years there has been an explosion of interest in mixed valency chemistry, ranging from preparative inorganic and organometallic chemistry, through the

physical chemistry of electron transfer processes, into the solid state physics of one-dimensional metals, and in other quite disparate directions such as biology and mineralogy. The present article aims to give a synoptic view of these new developments, taking account of advances in theory, in the results of new physical measurements and in the elucidation of new types of mixed valency compound, most of which did not exist in 1967. It is certainly not comprehensive, and very likely is biased. For much greater detail on particular aspects, the Proceedings of a NATO Advanced Study Institute entitled 'Mixed Valency Compounds' (Brown, 1980) should be consulted, while for brief and popular accounts, see articles by the present author in *Endeavour* (1970), *La Recherche* (1981) and *Comments on Inorganic Chemistry* (1981). There have also been a number of review articles on specific aspects of mixed valency chemistry, such as the coupling mechanisms in binuclear Ru(II,III) and other complexes, organometallic compounds, intervalence optical transitions in minerals and one-dimensional compounds. A selection from these is listed separately from the main body of references at the end of this article, to give an entry into the now very extensive primary literature. In what follows, we shall first describe some of the recent theoretical approaches to the statics and dynamics of intervalence interactions and then summarize the present state of knowledge about particular categories of mixed valency compound.

THEORIES OF MIXED VALENCY

Preliminaries

In Fig. 1 is shown a schematic picture of the most general kind of mixed valency situation. Two neighbouring metal ions A and B, each surrounded by a coordination environment which may consist of similar or different numbers and types of ligand, are connected by a pathway often consisting of a common ligand. A and B ions are of the same element but, on a time-scale to be discussed, have different oxidation states.

$$
\begin{array}{ccc}
A & L & B \\
Fe^{II} & O^{2-}; Cl^- & Fe^{III} \\
Ti^{III} & CN^- & Ti^{IV}
\end{array}
$$
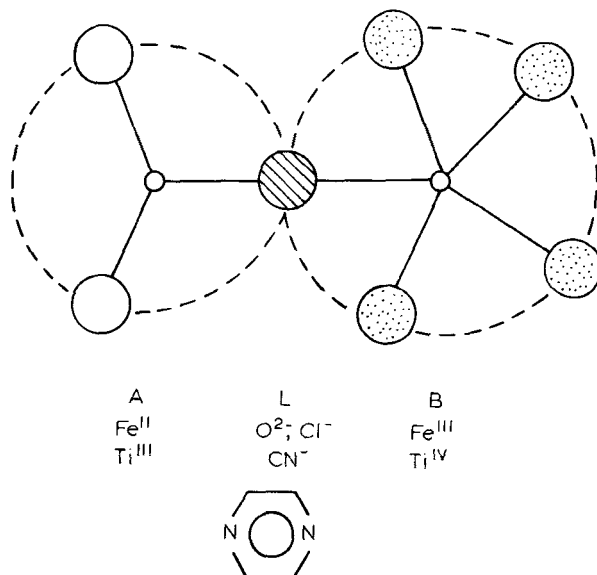
FIG. 1. Schematic view of two mixed valency ions with their ligand environments and a bridging group.

FIG. 2. Elements forming mixed valency compounds. with oxidation states.

Elements known to form at least one mixed valency compound are displayed in Fig. 2, with the combinations of oxidation state most commonly found. Over a third of the Periodic Table is represented, with the bulk of the examples concentrated, not very surprisingly, in d- and f-block elements. Numerous cases also exist among the B-subgroups, where the Group oxidation state N often co-exists with (N-2). Bridging ligands in Fig. 1 range from monoatomic anions like O^{2-}, or Cl^- through diatomic (CN^-) to bifunctional aromatic molecules like pyrazine, 4,4'-bipyridyl and others even more elaborate, some of which are listed later (Table 3).

In terms of their stoichiometry two types of mixed valency compound can be distinguished. On the one hand are those in which an element clearly has a non-integral average oxidation state, on the ground of stoichiometry alone, e.g. Fe_3O_4, where (since the most loosely bound electrons are certainly largely of Fe 3d type) the choice is to have 5.33 d-electrons on each Fe, or 6 on one and 5 on the other two. However, quite a lot of mixed valency compounds have an apparently integral average oxidation state, though one which would be very unusual for the element in question, e.g. $Pt(NH_3)_2Cl_3$ or SbO_2. Here there are other structural and physical grounds for believing that we do not, in any sense, have Pt(III) and Sb(IV), but Pt(II,IV) and Sb(III,V). It is also important at the outset to realize that what we are calling 'mixed valency' here is quite a different phenomenon from the one which many physicists recently call by the same name, that is, the fluctuation of electron configuration between say $4f^6$ and $4f^5 5d^1$ in such purely stoichiometric compounds as SmS (*see* e.g., Campagna *et al.*, 1974).

In deciding on the most appropriate theoretical format for describing the electronic states, and hence the physical and chemical properties, of mixed valency systems a couple of preliminary points need clearing up.

1. How should we treat electron exchange between the two centres? If the intervalence interaction were weak we could treat it as a perturbation on the single valence wave-functions, as in the valence-bond approximation. The ground state might then be written as $(Fe_A^{II}F_B^{III} + \lambda Fe_A^{III}Fe_B^{II})$ for example, where A and B are the two sites in Fig. 1 and λ is small. In fact that was the starting point of our own model (Robin and Day, 1967). On the other hand if electron exchange between A and B were a dominant feature one would move to the molecular orbital limit and construct LCAO one-electron wavefunctions from Fe 3d orbitals, or tight-binding band functions in the case of continuous solids. It is precisely because examples exist in mixed valency chemistry covering both these limiting cases, and all stages in between, that the field has proved so fascinating.

2. Do we aim at a static or a dynamic model? In some mixed valency systems electron exchange is slow enough on the time-scale of the vibrational motion that one can treat the electrons as trapped, and consider the wavefunctions appropriate to a fixed static nuclear framework. On the other hand, as we shall illustrate later, there are certainly cases where the 'extra' electron exchanges between the two centres of differing oxidation state on a time-scale comparable to that of a molecular skeletal vibration, and in which, therefore, the nuclear and electronic motions are inextricably connected, i.e. we have *par excellence* systems where the Born–Oppenheimer approximation does not apply.

The Robin–Day model

It was a static model which formed the basis of the Robin–Day (RD) classification scheme. Suppose the oxidation states of ions at A and B in Fig. 1 are n and $n + 1$. A first approximation to the ground state might be $\Psi_0 = A^n B^{n+1}$. But if the ligand fields around

the two sites are quite similar (though distinguishable) the valence bond configuration $\Psi_1 = A^{n+1}B^n$ will not have a very much greater energy than Ψ_0. If there exists a suitable perturbation matrix element to mix them together the correct ground state wavefunction is the combination

$$\Psi_G = (1 - \alpha^2)^{1/2}\,\Psi_0 + \alpha\Psi_1. \tag{1}$$

The magnitude of the 'valence delocalization coefficient' α is determined by the energy $E_1 = \langle \Psi_1 | \mathscr{H} | \Psi_1 \rangle$ of Ψ_1 relative to Ψ_0 and the off-diagonal matrix element $V_{01} = \langle \Psi_0 | \mathscr{H} | \Psi_1 \rangle$ which mixes the two configurations together. Focusing first on E_1, it is clear that for a one-electron transfer between A and B, only a difference between the ligand fields round the two sites can lead to $E_1 \neq 0$, because in the gas phase the ionization potential $A^n \to A^{n+1}$ is equal and opposite to the electron affinity $B^{n+1} \to B^n$. Thus the more different the sites are in geometry, in ligands or in bond lengths the larger is E_1 and the smaller is α. Compounds in which the sites are so different that α is negligible are called class I, while ones which have similar, but still distinguishable sites are class II. If we know from the stoichiometry that the average oxidation state is non-integral, but find all the metal ion sites crystallographically indistinguishable, α takes its maximum value (class III). Some examples of the three classes are given in Table 1.

As far as physical properties are concerned, in class I all properties determined by local forces, e.g. core-shell photoionization energies, Mössbauer chemical shifts, etc. are just a superposition of those of the two oxidation states taken separately. Direct optical transitions $E_0 \to E_1$ are at very high energy, and likewise thermally activated electron transfer requires too great an energy to observe conductivity in the solid state.

In class II compounds α has a small but finite value so 'local' properties are still close to those of the individual single oxidation states. However, optical transitions $E_0 \to E_1$ now

TABLE 1. Some examples of the three Robin–Day classes of mixed valency compound

	Site A	Site B	Formal oxidation states	
			A	B
Class I				
Sb_2O_4	Distorted tetrahedral Av.Sb–O 2.13 Å	Octahedral Sb–O	III	V
$GaCl_2$	Distorted 8-coord Ga–Cl 3.2 Å	Tetrahedral Ga–Cl 2.19 Å	I	III
Class II				
V_7O_{13}	Octahedral V–O 1.964 Å	Octahedral V–O 1.945 Å	III	IV
$Fe_4[Fe(CN)_6]14H_2O$	Octahedral Fe–C 1.92 Å	Octahedral Fe–N 2.03 Å	II	III
$(NH_4)_2SbBr_6$	Octahedral Sb–Br 2.795 Å	Octahedral Sb–Br 2.564 Å	III	V
$Mn_2O_2(bipy)_4^{3+}$	Distorted octahedral Av.Mn–N 2.174 Å	Distorted octahedral Av.Mn–N 2.048 Å	III	IV
Class III				
Na_xWO_3	Octahedral Av. W–O 2.1 Å	Octahedral	VI–V	VI–V
$Fe_4S_4(SCH_2Ph)_4^{2-}$	Tetrahedral Av. Fe–S 2.277 Å	Tetrahedral	2.5	2.5
$K_2Pt(CN)_4Br_{0.30}3H_2O$	Planar Pt–Pt 2.89 Å	Planar	2.30	2.30

appear at lower energy, often in the visible, giving the bright colours so characteristic of many mixed valency compounds. Such compounds are also semiconductors.

If they are continuous lattice solids class III compounds are expected to be metallic, since the 'extra' electrons are spread out over all sites with equal probability, and they will have no 'local' properties characteristic of the integral oxidation states n, $n + 1$ but of something intermediate. On the other hand numerous discrete metal clusters are of class III type but cannot, of course, be metallic since intercluster electron hopping is not favoured. Their excited states, too, do not form a continuous band but are found at discrete energies corresponding to electronic transitions between molecular orbitals delocalized over the cluster.

A perturbation model for bridging groups

The utility of the simple static RD model has been demonstrated by applying it to a very large number of compounds. We have not, however, mentioned the role of V, which emphasizes the part played by the intervening ligands in the interaction. In most mixed valency compounds A and B are at least 5–6 Å apart so direct overlap between, e.g., d-orbitals on each centre must be very small. Consider two such orbitals χ_A, χ_B separated by a bridging ligand L with highest occupied and lowest unoccupied orbitals ϕ_L and ϕ_L^*. Suppose (Mayoh and Day, 1972, 1973) that the ground state mixed valency configuration is $\phi_L^2 \chi_A^2 \chi_B^1 (\Psi_0)$ and the intervalence charge transfer excited state $\phi_L^2 \chi_A^1 \chi_B^2 (\Psi_1)$. Assuming zero differential overlap $V_{01} \sim \langle \chi_A | \mathscr{H} | \chi_B \rangle \sim 0$. Any interaction between Ψ_0 and Ψ_1 must therefore take place via interaction with 'local' charge transfer configurations such as $\phi_L^1 \chi_A^2 \chi_B^2 (\Psi_2)$ or $\phi_L^2 \chi_A^1 \chi_B^1 \phi_L^{*1} (\Psi_3)$. Normally these lie higher in energy than Ψ_1 but have much larger matrix elements V_{02}, V_{03}, V_{12} and V_{13} than V_{01}. Second-order perturbation theory gives

$$\alpha = \sum_{n=2,3} (V_{0n} V_{1n})/(E_1 - E_0)(E_n - E_0) \tag{2}$$

$$\beta = \sum_{n=2,3} - (V_{0n} V_{1n})/(E_1 - E_0)(E_n - E_1) \tag{3}$$

where β is the excited state valence delocalization coefficient in

$$\Psi_E = (1 - \beta^2)^{1/2} \Psi_1 + \beta \Psi_0. \tag{4}$$

It is also possible to extend the summation over all configurations of the type $\chi_A \to \phi_{Lj}^*$ and $\phi_{Lk} \to \chi_B$. The many-electron matrix elements V_j can be expressed in terms of one-electron matrix elements which, in turn, become metal-ligand resonance integrals. The latter may be evaluated from appropriate atomic wavefunctions using the Linderberg method or, more empirically, chosen to reproduce the observed oscillator strengths of identifiable $\chi_A \to \phi_L^*$ and $\phi_L \to \chi_B$ transitions, either in the mixed valency complex itself or in the corresponding monomeric single valency fragments. In any case it is best to take the E_n where possible from the measured absorption peaks. Proceeding in this way values of α of the magnitude 10^{-1} have been obtained for several typical bridged class II complexes such as Prussian Blue and the related dimer $[(NC)_5 Fe(CN)Fe(CN)_5]^{6-}$ and somewhat smaller ones (3×10^{-2}) for Fe(II,III) compounds bridged by oxide ions (e.g. biotite micas), where the $\chi_A \to \phi_L^*$ charge transfer states lie at very high energy. The calculated values are validated by comparing the oscillator strength of the $\Psi_0 \to \Psi_1$ intervalence transition obtained from them with the observed ones. Agreement for strongly trapped class II systems is quite good (Mayoh and Day, 1973; Richardson, 1981).

Other experimental measures of α are ones which observe the degree of spin transfer from A to B in the ground state, for example transferred hyperfine interactions in Mössbauer spectroscopy or, even more directly, the magnetization density distribution found by polarized neutron diffraction (Day *et al.*, 1980). In the case of Prussian Blue both methods agree on an upper limit of 10^{-1} for α, but unfortunately were not sensitive enough to give a precise value.

Dynamics of electron transfer: adiabatic and Franck–Condon processes

Although the static model just described gives quite a satisfying picture of intervalence charge transfer mixing in terms of the energy difference between E_0 and E_1 and the magnitude of V_{01}, there is plenty of evidence that coupling between the electronic and vibrational motion has fundamental importance in both thermal and optical intervalence transfer. Most immediately obvious is the fact that intervalence optical transitions invariably have a very large Franck–Condon width, full widths at half height of 5000 cm^{-1} being by no means exceptional. Thus, the relaxed excited state is displaced very far from the minimum in the ground state potential energy surface. In fact, as Hush (1967) pointed out, the relaxed excited state after a one-electron intervalence transfer is electronically very similar to the original ground state, and most of the energy of the optical transition goes into vibrational excitation. For instance in a transfer

$$\text{Fe}_A^{II}L_n + \text{Fe}_B^{III}L'_{n'} \rightarrow \text{Fe}_A^{III}L_n + \text{Fe}_B^{II}L'_{n'} \tag{5}$$
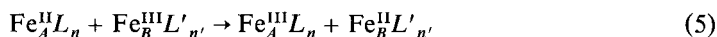
the only electronic contribution comes from the difference in the ligand fields exerted by L and L', just as in the RD model. Assuming harmonic potentials the most general situation is as shown in Fig. 3 where the left-hand potential surface represents the variation with the vibrational coordinates of the electron configuration on the left-hand side of Eq. (5) and
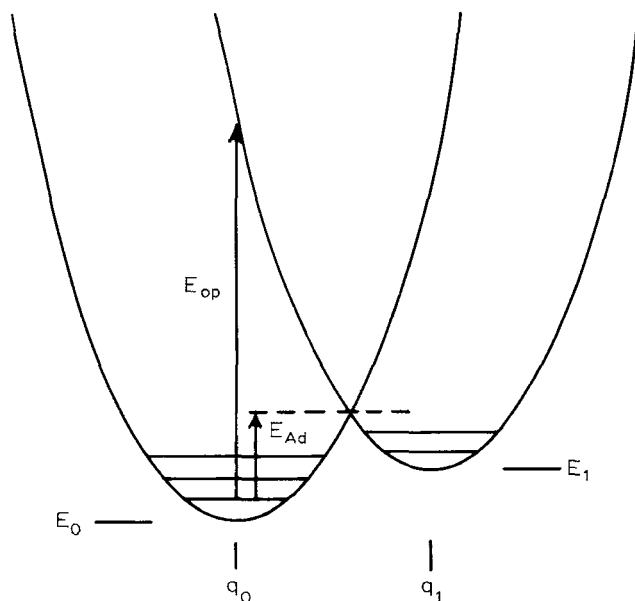

FIG. 3. Potential energy surfaces of Ψ_0 and Ψ_1 (defined in the text). E_{op} and E_{Ad} are the optical (Franck–Condon) and adiabatic intervalence electron transfer energies.

the right surface that on the right-hand side of Eq. (5). The vertical line E_{op} is the Franck–Condon maximum of the optical intervalence transition while E_{Ad} is the energy of a thermally activated electron transfer. In the case that $(q_1 - q_0)$ was small compared to $(E_1 - E_0)$ we would return towards the RD static limit but if the mixed valency complex were symmetrical $(L = L', \; n = n'$ in Eq. (5)) one would have the simple geometrical relationship

$$E_{op} = 4E_{Ad}. \tag{6}$$

Very few direct tests of Eq. (6) have been made because the activation free energy measured from the rate of a self-exchange process like (5) taking place in solution includes contributions from other processes such as the energy required to bring the reactants together and reorganize the solvent. If adiabatic electron transfer could be observed in the solid state this problem would be circumvented but only one study of a direct comparison between semiconduction activation energy and optical intervalence frequency appears to have been reported (Culpin *et al.*, 1965, 1968). In that case, a series of chlorocuprate(I,II) salts, E_{op} was 17 500 cm^{-1} while E_{Ad} was 6000 cm^{-1}.

Clearly, however, neither Franck–Condon nor adiabatic electron transfer can take place between A and B if the two surfaces in Fig. 3 are orthogonal. In the vicinity of the intersection there must be an 'avoided crossing' brought about by a matrix element like V_{01}. The situation is no longer a static one and the relevant matrix element is a function of the vibrational as well as the electronic coordinates. If we invoke the Born–Oppenheimer approximation, $\Psi_{0i} = \psi_0 \chi_{0i}$ and $\Psi_{1j} = \psi_1 \chi_{1j}$ where the ψs are the electronic functions and χs the vibrational ones. Then

$$V_{0i,1j} = \langle \psi_0 \chi_{0i} | \mathcal{H} | \psi_1 \chi_{1j} \rangle = V \langle \chi_{0i} | \chi_{1j} \rangle. \tag{7}$$

Application of time-dependent perturbation theory leads to the result that the rate of transition from Ψ_{0i} to any of the vibrational levels χ_{1j} of Ψ_1 is

$$W_{0i} = (2\pi/\hbar) V^2 \langle \chi_{0i} | \chi_{1j} \rangle^2 \rho(E_{0i} = E_{1j}) \tag{8}$$

where ρ is the density of vibrational levels in the state near the energy E_{0i}. This is the so-called Fermi 'Golden Rule'. The total transition probability W_{0i}, proportional to the rate-constant for crossing between the two potential energy surfaces of Ψ_0 and Ψ_1 is then obtained by making a thermal average over all the vibrational levels χ_{0i} which have the greatest overlap with the χ_{1j} having the same energy, $E_{0i} = E_{1j}$. That can only be those vibrational levels lying at, or close to, the crossing point between the two potential energy surfaces. To carry out the summations involved in evaluating W_{01}, it is normally assumed that the energy intervals between the vibrational levels are small enough to use a semi-classical treatment (e.g. Levich, 1970). Then the total adiabatic transition probability is given by

$$W_{01} = (2\pi/\hbar) V^2 [\pi/kT(E_{op} - E_1)] \exp(-E_{Ad}/kT). \tag{9}$$

The formidable list of assumptions used to derive this expression are:

1. Weak electronic coupling.
2. Harmonic potential energy surfaces.
3. Identical normal mode frequencies in both potential energy surfaces.
4. Strong vibrational-electronic interactions.
5. Vibrational intervals which are much smaller than kT.

Equation (9) is already familiar from theories of the rates of electron transfer reactions in solution but Meyer (1979), in particular, has pointed out a great advantage which mixed-valency dimers have over collision complexes in solution when attempts are made

to estimate the various quantities which enter the equation. Meyer's principal point is that the frequency and intensity of the optical intervalence transition carry information respectively on E_{Ad} and V_{01}. In the symmetrical case ($E_0 = E_1$ in Fig. 3) Eq. (6) applies, or otherwise

$$E_{Ad} = E_{op}^2/4[E_{op} - (E_1 - E_0)].$$ (10)

Assuming zero overlap between donor and acceptor orbitals the transition dipole moment of the intervalence absorption $\Psi_G \rightarrow \Psi_E$ (Eqs. (1) and (4)) is

$$M_{GE} = \langle \Psi_G \mid er \mid \Psi_E \rangle = \tfrac{1}{2}e(\alpha + \beta)\,R$$ (11)

where R is the distance between the sites A and B and V_{01} can then be evaluated from the experimental values of α and β, for example, via Eqs. (2) and (3). Some numerical values of W_{01} estimated from intervalence absorption spectra are given in Table 2. They refer to acetonitrile at 23°C, and appear to have quite reasonable orders of magnitude compared with outer-sphere self-exchange reactions of the corresponding monomeric Ru^{II} and Ru^{III} complexes.

TABLE 2. Values of W_{01} (eq. (9)) in acetonitrile at 23°C calculated from the properties of intervalence optical transitions of $[(bipy)_2ClRu^{II}(L)Ru^{III}(bipy)_2Cl]^{3+}$ (Meyer, 1979)

L	E_{op} (eV)	E_{Ad} (eV)	V_{01} (eV)	W_{01} (s^{-1})
pz	0.95	0.24	0.049	2.4×10^{10}
4,4'-bipy	1.26	0.32	0.017–0.025	$(1.0–2.8) \times 10^8$
BPE	1.34	0.34	0.016–0.023	$(5.1–10) \times 10^7$

A complication arising from attempts to estimate adiabatic electron transfer rates from optical data for mixed valency dimers concerns the respective contributions of intra-molecular skeletal vibrational modes and solvent reorganization to E_{Ad}. For solvent vibrations, assumption (5) above is very likely to be correct, but much less likely so for molecular vibrations, which may have frequencies above 200 cm^{-1}. One method which has been proposed for separating the two contributions is to measure the frequency of the intervalence band E_{op} as a function of solvent dielectric constant since the variation should be entirely the result of the solvent reorganization (Tom et al., 1974). In the dielectric continuum approximation (Marcus, 1956, 1965; Hush, 1961) the contribution E_s to E_{op} from solvent reorganization is

$$E_s = e^2\left(\frac{1}{2a_A} + \frac{1}{2a_B} - \frac{1}{d}\right)\left(\frac{1}{D_{op}} - \frac{1}{D_s}\right)$$ (12)

if the charge distributions around the two sites A, B are assumed to be spheres of radius a_A, a_B with centres separated by d. D_{op} and D_s are the optical and static dielectric constants. Some examples of the application of Eq. (12) are given below. A better approximation than a pair of charged spheres is a charged ellipsoid, as treated originally by Kirkwood and Westhemer (1938) and applied to mixed valency dimers by Cannon (1977). It is also worth noting in passing that Eq. (12) also contains a simple prediction about the distance dependence of E_{op}, which has been verified for a series of $Ru^{II,III}$ dimers bridged by ligands of increasing length (Powers et al., 1976), and also in some biferrocenium ions (Powers and Meyer, 1978). It has also been found recently to apply to shifts in intervalence absorption bands in crystals on lowering the temperature from 300 to 4 K, as a result of contracting the lattice (Prassides, 1980).

Building on the theories developed originally to describe the interaction of point defects in crystals with localized and lattice vibrations (e.g. Huang and Rhys, 1951), the frequencies of the skeletal modes which couple to mixed valency electron transfer can also be estimated by measuring the temperature dependence of the intervalence absorption band profile. Because the relaxed excited state in an intervalence transition (q_1 in Fig. 3) lies very far from the ground state q_0 in the configuration coordinate diagram, such absorption bands are always very wide, and do not become dramatically narrower on cooling. In particular, no vibrational fine-structure has ever been observed in an intervalence band. Quite generally the shape function $G(\nu)$ of a broad absorption band is given by the sum of terms involving the overlap integrals between all the vibrational wavefunctions χ_{oi} in the ground state Ψ_0 and χ_{1j} in the excited state Ψ_1 weighted by the thermal occupancy $P(i)$ of χ_{oi} (e.g. Markham, 1959):

$$G(\nu) = \sum_{ij} P(i) \langle \chi_{oi} | \chi_{1j} \rangle^2 \, \delta[\nu - (E_{1j} - E_{0i})/\hbar] \qquad (13)$$

$$P(i) = \prod \left\{ \exp\left(\frac{-i\hbar\omega_0}{kT}\right) \left[1 - \exp\left(\frac{-\hbar\omega_0}{kT}\right) \right] \right\} \qquad (14)$$

if the force field is harmonic

$$E_{0i} = E_0 + \hbar\omega_0(i + \tfrac{1}{2})$$
$$E_{1j} = E_1 + \hbar\omega_1(j + \tfrac{1}{2}) \qquad (15)$$

where ω_0 and ω_1 are vibrational frequencies in states 0 and 1. Of course, there may be many modes in both states but we assume for simplicity that there is only one 'effective' mode. If it is further assumed that $\omega_0 = \omega_1$ then $G(\nu)$ is a Gaussian with a halfwidth H given by

$$H^2 = 8(\ln 2) \, \hbar^2 \, \omega^2 \, S \, \coth(\hbar\omega_0/2kT) \qquad (16)$$

where S is the Huang–Rhys factor, the ratio between the vibrational energy excited in the upper state to the energy of a single vibrational quantum

$$S = (1/2) \, \omega_0^2 (q_1 - q_0)^2/\hbar\omega. \qquad (17)$$

Equations (16) and (17) are equivalent to assuming that one can neglect quantization of the vibrations in the upper state so that there is a continuum of upper state vibrational levels so the probability of a Franck–Condon transition from the ground state is proportional to $|\chi_0|^2$. Equation (16) was first investigated experimentally for mixed valency compounds by Atkinson and Day (1969), who found a good fit was obtained for $\omega = 210$ cm^{-1} and $S = 130$ in the Sb^{III} → Sb^V transition in crystals of $(CH_3NH_3)_2$-Sb$_{1-x}$Sn$_x$Cl$_6$. Analogous measurements on $[(CN)_5Fe(pyrazine)Fe(CN)_5]^{5-}$ (Felix and Ludi, 1978) and Prussian Blue (Ludi, 1980) yielded values of $\omega = 490$ and 430 cm^{-1} (Fig. 5). Clearly these figures lie within the range expected for metal-ligand stretching vibrations, but only in the case of the Sb^{III,V} system was it possible to make a direct comparison with known normal mode frequencies. In that example the intervalence transition is

$$Sb_ACl_6^{3-} + Sb_BCl_6^- \rightarrow Sb_ACl_6^{2-} + Sb_BCl_6^{2-} \qquad (18)$$
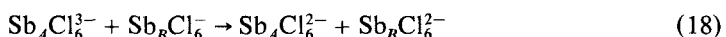
and it is known from the crystal structures of related compounds (Lawton and Jacobson, 1966; Birke, Latscha and Pritzkow, 1976) that the SbCl$_6$ units approximate very closely to octahedra in both oxidation states, with a bond length difference of 0.1–0.3 Å. The a_{1g} stretching modes of the Sb(III) and Sb(V) have frequencies of 267 and 329 cm^{-1} respectively (Barrowcliffe *et al.*, 1967), i.e. both higher than the effective frequency broadening
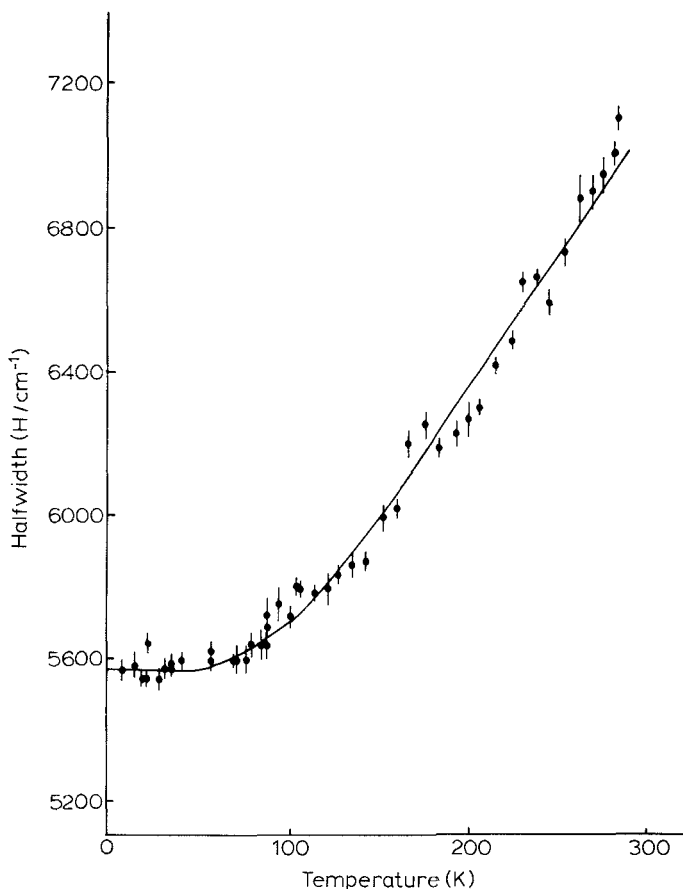
FIG. 4. Halfwidth of the intervalence electron transfer band in $(CH_3NH_3)_2$-$Sb_{1-x}Sn_xCl_6$ as a function of temperature. The full line is calculated from Eq. (16) with $\omega = 234$ cm^{-1} (Prassides, 1980).

the intervalence absorption band. However, there is no direct evidence about the extent to which each individual mode of the two octahedra couples to the electronic transition. In fact, if the assumption is made that all internal modes contribute equally, weighted only by their degeneracy, the resulting averages (163 cm^{-1} for $SbCl_6^{3-}$ and 249 cm^{-1} for $SbCl_6^-$) fall on either side of the 'effective' frequency observed. A better assumption would be that there are two 'effective' ground state frequencies, one for each ion, and that the effective excited state vibrational frequency was not necessarily equal to that of the ground state. Under these circumstances Markham (1959) showed that the half-width of the absorption band (strictly speaking, the second moment) was

$$H^2 = \hbar^2\, \omega_1^2(A)\, S_A \coth(\beta_A/2) + \hbar^2\, \omega_1^2(B)\, S_B \coth(\beta_B/2) \qquad (19)$$

where

$$\beta_A = (\hbar/kT)\, \omega_0(A); \quad \beta_B = (\hbar/kT)\, \omega_0(A) \qquad (20)$$

and A and B refer to the two ions. If we take $\omega_0(A)$ and $\omega_0(B)$ as 163 and 249 cm^{-1} and $\omega_1(A) = \omega_1(B) = \omega_1 = (1/2)(\omega_0(A) + \omega_0(B))$, because the two relaxed excited state ions
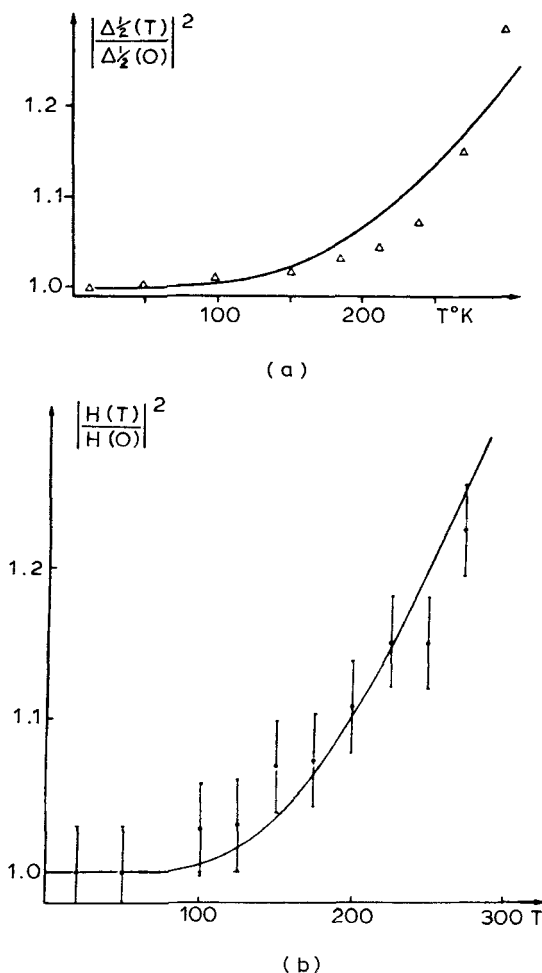
(a)

(b)

FIG. 5. Temperature variation of halfwidths of intervalence bands in (a) $[(CN)_5Fe(pz)Fe(CN)_5]^{6-}$ (Felix and Ludi, 1978) and (b) Prussian Blue (Ludi, in Brown, 1980). The full lines are calculated from Eq. (16) with $\omega = 490$ and 430 cm^{-1} respectively.

on the righthand side of Eq. (18) are identical, the limiting halfwidth of the Gaussian band at 0 K is

$$H(O)^2 = 8(\ln 2)\, \hbar^2\, \omega_1^2(S_A + S_B). \tag{21}$$

Experimentally $H(O)$ is 5550 cm^{-1} (Prassides, 1980) which, taking into account the reduced masses associated with all the modes, yields an estimate of 0.3 Å for the difference between the bond lengths of SbCl$_6^{3-}$ and SbCl$_6^{-}$ in their ground states, in quite good agreement with what is observed (Fig. 4).

Class II or class III dimers: V_{01} versus E_{Ad}

There can be no doubt that the very large width and lack of resolved vibrational structure in intervalence charge transfer spectra is the result of the large changes of
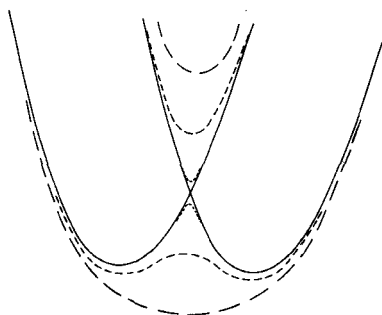
FIG. 6. Potential energy surfaces for a symmetrical mixed valency dimer. The dotted, short dashed and long dashed lines represent the surfaces for $E_{Ad} \gg V_{01}$, $E_{Ad} \sim V_{01}$ and $E_{Ad} \ll V_{01}$ (see text).

bond lengths taking place when electrons are transferred into and out of a localized orbital. In strongly trapped class II examples there is only very limited mixing between the donor and acceptor wavefunctions so the 'avoided crossing' at the intersection of the two potential energy surfaces in Fig. 3 is a small perturbation and the semiclassical theories we have just described cope quite satisfactorily with the main experimental characteristics of both adiabatic and Franck–Condon electron transfer. On the other hand there is no reason *a priori* why V_{01} should be small compared with E_{Ad}, a thought which was highlighted in a particularly stark fashion by the preparation of the dimeric cationic complex $[(NH_3)_5Ru(pyrazine)Ru(NH_3)_5]^{5+}$, now known as the Creutz–Taube (CT) complex (Creutz and Taube, 1969). In this ion each Ru has a distorted octahedral ligand field exerted by five NH_3 nitrogen atoms and one nitrogen from the pyrazine so as far as the ligand environments are concerned the two Ru could be identical. Whether they are or not remains controversial and the evidence is reviewed later, but in related ions containing bipyridyl and Cl in place of the NH_3 it seems clear that there is no inversion centre (Powers *et al.*, 1976).

With identical ligands around each metal ion it might be thought that the complex would inevitably belong in class III of the RD classification. However, it was first pointed out by Mayoh and Day (1972) how it might still be possible for such a complex to be in class II if the vibrations of the ligands around the sites A and B were taken into account. To each wavefunction Ψ_0, Ψ_1 defined in the RD static model corresponds a potential energy surface. As shown in Fig. 6 they are identical, but displaced along the normal coordinate which carries the equilibrium configuration of $A^n B^{n+1}$ to $A^{n+1}B^n$. The mixing between these two surfaces via the matrix element V_{01} produces two new ones separated, as shown, by $2V_{01}$. If $V_{01} \ll E_{Ad}$ the lower surface retains two minima close to the positions in the configuration coordinate space which they would have occupied in the absence of the interaction. Thus the minimum of energy corresponds to an unsymmetrical valence distribution. In contrast, if $V_{01} \gg E_{Ad}$ there is now a single minimum in the lower potential energy surface at a symmetrical configuration, so we have a qualitative criterion for localization or delocalization. For the model case of two orthonormal electron wavefunctions linearly coupled to a doubly degenerate vibration the quantitative criterion for localization is $V_{01} < 2E_{Ad}$ (Hush, 1975).

The Piepho–Krausz–Schatz model

Figure 6 makes it clear that there is a strong analogy between the potential energy surfaces of a dimeric mixed valency complex and those generated by the interaction of a doubly

degenerate electronic state with a vibrational mode, i.e. the Jahn–Teller effect. The main difference, of course, stems from the fact that the electronic degeneracy in the mixed valency problem is associated with oscillations of an electron between two orbitals centred on different atoms, while Jahn–Teller degeneracy is about a single centre. Piepho, Krausz and Schatz (PKS) (1978) recently worked out the vibronic problem explicitly for the mixed valency case and derived eigen values and vibronic coefficients using a formalism originally developed by Fulton and Gouterman (1961) to describe the excited states of symmetrical dimers such as $(C_6H_6)_2^+$. Defining Ψ_0 and Ψ_1 in the same way as we did in the RD static model, they use the harmonic approximation and consider only the totally symmetric normal coordinates Q_A, Q_B of each subunit. The vibrational potential energy of A in oxidation state n is

$$W_n^A(Q_A) = W_n^0 + L_n^A Q_A + (1/2) k_n^A Q_A^2 \tag{22}$$

and similarly for W_{n+1}^A, W_n^B and W_{n+1}^B. Putting $k_n^A = k_n^B = k_n$, etc.,

$$W_0 = W_n^A(Q_A) + W_{n+1}^B(Q_B) = lQ_A + (1/2) k_n Q_A^2 + (1/2) k_{n+1} Q_B^2$$

$$W_1 = W_{n+1}^A(Q_A) + W_n^B(Q_B) = lQ_B + (1/2) k_{n+1} Q_A^2 + (1/2) k_n Q_B^2. \tag{23}$$

If one introduces new vibrational coordinates

$$Q_\pm = (1/\sqrt{2})(Q_A \pm Q_B) \tag{24}$$

and makes the rather drastic assumption that $k_n = k_{n+1} = k$

$$W_0 = (1/\sqrt{2}) lQ_- + (1/2) kQ_-^2 + (1/\sqrt{2}) lQ_+ + (1/2) kQ_+^2$$

$$W_1 = (-1/\sqrt{2}) lQ_- + (1/2) kQ_-^2 + (1/\sqrt{2}) lQ_+ + (1/2) kQ_+^2 \tag{25}$$

the problem is separable into Q_+ and Q_- (or q) terms, of which only the latter is important for spectroscopic and other properties connected with intervalence transfer. PKS now define dimensionless variables

$$q = 2\pi(v_-/h)^{1/2} Q_-; \quad \lambda = (8\pi^2 hv_-^3)^{-1/2} l \tag{26}$$

whence

$$W_0/hv_- = \lambda q + (1/2) q^2; \quad W_1/hv_- = -\lambda q + (1/2) q^2. \tag{27}$$

The next stage is to allow A and B to interact via V_{01} so that new wavefunctions such as Ψ_G and Ψ_E (Eqs. (1) and (4)) are generated, but it is important to note that V_{01} is now a function of both the electronic and vibrational coordinates around A and B. In fact, to make the problem tractable it has to be assumed that $V_{01} = V_{01}^0$, its value when all the nuclei are fixed at their equilibrium configurations. A further parameter to describe the electronic coupling is now defined as

$$(hv_-) \varepsilon = V_{01}^0 \tag{28}$$

so first-order perturbation theory yields the secular determinant

$$\begin{vmatrix} \lambda q + (1/2) q^2 - W_k & \varepsilon \\ \varepsilon & -\lambda q + (1/2) q^2 - W_k \end{vmatrix} = 0 \tag{29}$$

$$\Psi_k = c_0 \Psi_0 + c_1 \Psi_1 \tag{30}$$

whence

$$W_{0,1} = (1/2) q^2 \mp (\varepsilon^2 + \lambda^2 q^2)^{1/2}. \tag{31}$$

For an unsymmetrical complex (RD class II) $W_n^A \neq W_n^B$ and $W_{n+1}^A \neq W_{n+1}^B$ so, defining one extra parameter W, roughly related to $E_1 - E_0$ in Fig. 3, to take account

of the difference between the minima in the two originally non-interacting potential energy surfaces,

$$W_{0,1} = (1/2)\, q^2 \mp [\varepsilon^2 + (\lambda q + W)^2]^{1/2}. \tag{32}$$

To emphasize the relationship between the RD and PKS models (Wong, Schatz and Piepho, 1979), one can write the PKS wave functions corresponding to the RD Ψ_G, Ψ_E of Eqs. (1) and (4) in the static limit (zero nuclear kinetic energy) as

$$\Psi_G^{PKS} = -(1/N\sqrt{2})[(\varepsilon - \kappa + \sigma)\,\Psi_0 + (\varepsilon - \kappa - \sigma)\,\Psi_1]$$
$$\Psi_E^{PKS} = (1/N\sqrt{2})[-(\varepsilon - \kappa - \sigma)\,\Psi_0 + (\varepsilon - \kappa + \sigma)\,\Psi_1] \tag{33}$$

where $N = [\sigma^2 + (\varepsilon - \kappa)^2]^{1/2}$, $\kappa = [\varepsilon^2 + \sigma^2]^{1/2}$, $\sigma = (\lambda q + W)$, all being functions of q. If q is set equal to λ there is a direct relationship with Eq. (1) such that

$$\alpha^2 = \tfrac{1}{2}\left[1 - \left(\frac{(\lambda^2 + W)^2}{\varepsilon^2 + (\lambda^2 + W)^2} \right)^{1/2} \right]. \tag{34}$$

In this equation, as W becomes large α tends to zero, exactly as in the RD model. The three RD classes I, II and III correspond respectively to the cases $|\varepsilon| \ll (\lambda^2 + W)$, $|\varepsilon| \lesssim (\lambda^2 + W)$ and $|\varepsilon| > (\lambda^2 + W)$. In a purely static model such as the RD one a complex in which $W = 0$ (or $E_1 = E_0$) could not be other than delocalized. The PKS model, on the other hand, taking account of the vibrational-electronic coupling, would allow such a complex to be localized or delocalized to an extent determined by the ratio $|\varepsilon|/\lambda^2$. The same point, though with somewhat different nomenclature, has also been made by Hush (1975).

Now it is most important to observe that although account has been taken of the interaction between the electronic wavefunctions and the vibrational motion, equations such as (30)–(33), not to mention earlier ones such as Eqs. (9) and (13), remain within the adiabatic Born–Oppenheimer approximation, that is, the nuclear kinetic energy has not yet been included in the Hamiltonian. To take advantage of the interchange symmetry $(A = B)$ it is convenient to use electronic functions $\Psi_\pm$ defined as

$$\Psi_\pm = (1/\sqrt{2})(\Psi_0 \pm \Psi_1) \tag{35}$$

and define a general vibronic function

$$\Phi_\nu (r, q) = \Psi_+(r)\,\chi_{+,\nu}(q) + \Psi_-(r)\,\chi_{-,\nu}(q) \tag{36}$$

where $\chi_\pm$ are also linear combinations of $\chi_{0,1}$. In the unsymmetrical case, where interchange symmetry is lost, the vibronic function is

$$\Phi_\nu(r, q) = \sum_{n=0}^{\infty} (c_{\nu n}\Psi_+ \chi_n + c'_{\nu n}\Psi_- \chi_n). \tag{37}$$

The intervalence band is now the envelope of all the transitions $\Phi_\nu \to \Phi_{\nu'}$, weighted by their differences in thermal population, as in Eq. (13). In the weak-coupling (class II) limit $\lambda^2 + W \gg |\varepsilon|$ it is found that the band should be gaussian, with a halfwidth (second moment) which varies with temperature according to a $\coth(h\nu_-/2kT)$ function as in Eq. (16). When the coupling $|\varepsilon|$ becomes stronger, and particularly in symmetrical complexes such as the CT ion the intervalence band becomes narrower and distinctly asymmetric. Observed and calculated band envelopes for the CT ion from the PKS model are shown in Fig. 7a and the corresponding potential energy surfaces in Fig. 7b. Agreement is quite good for values of ε and λ of -6 and 2.7 in units of a q quantum $\nu_- = 500$ cm^{-1}. On the other hand it has been suggested by Hush (1980) that symmetric expansion of the excited state ought to be taken into account in addition to the coupling to ν_-.
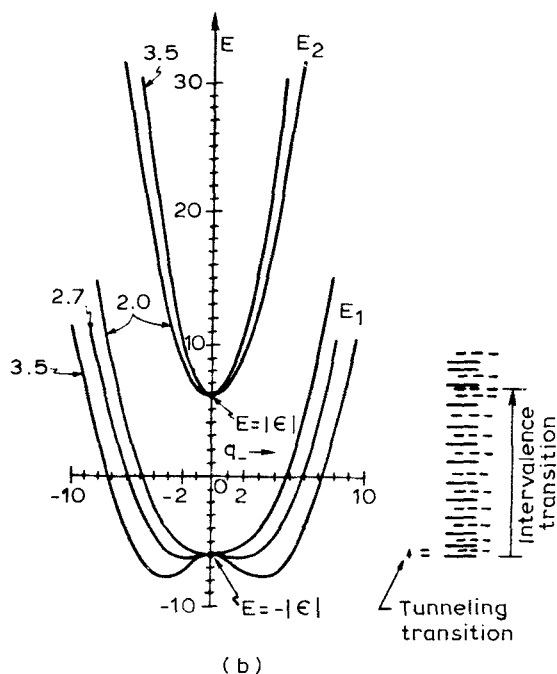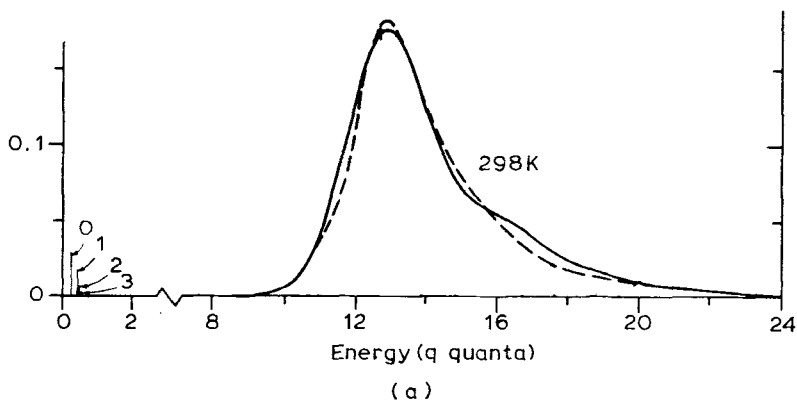
FIG. 7. The PKS model applied to the Creutz–Taube complex. (a) Observed (––––) and calculated (——) intervalence band profiles at room temperature. The calculation used $\varepsilon = -6$, $\lambda = 2.7$ (Piepho *et al.*, 1978). Also shown are the predicted infrared tunnelling transitions. (b) Potential energy surfaces calculated for $\varepsilon = -6$, $\lambda = 2.0, 2.7, 3.5$. The intervalence transition is shown for the $\lambda = 2.7$ case.

Adding a fourth parameter S to indicate the energy of coupling Shv_+ to the symmetric mode, assumed to have the same frequency as v_- Hush finds that he, too, can get reasonable agreement with the observed intervalence band shape for the CT ion (Fig. 8) but with parameter values suggesting a delocalized ground state, with a single minimum in the lower potential energy surface. Clearly this remains an open question (*see* later for further discussion of other experimental evidence about the CT complex) but it is worth noting that Hush's point may give the answer to a puzzling dilemma arising from
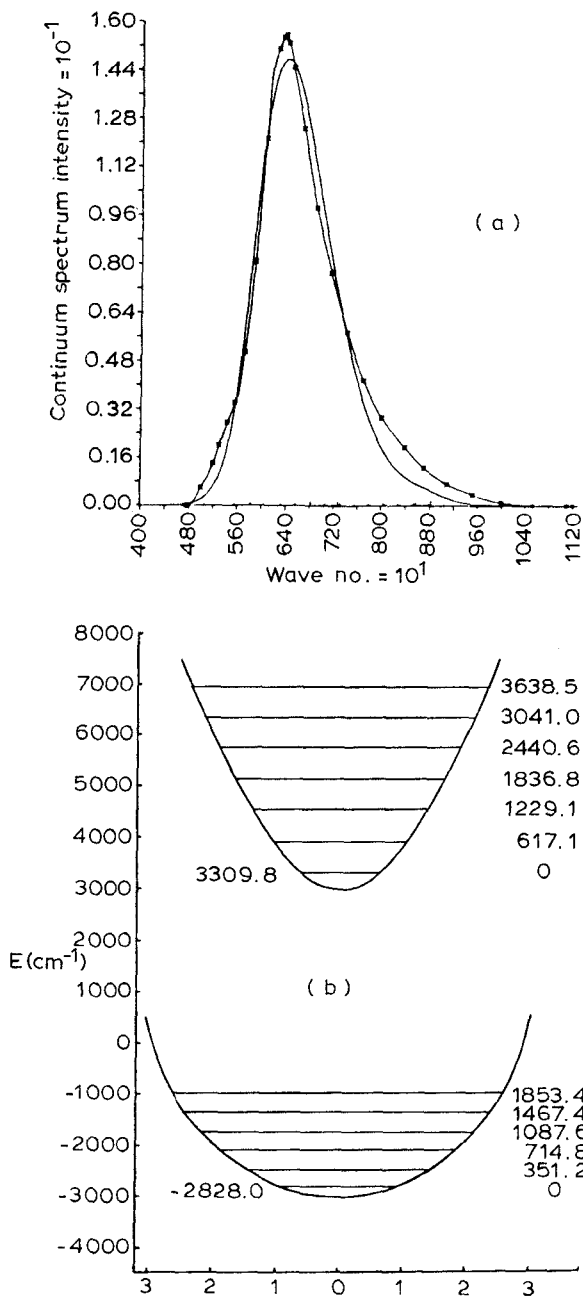
FIG. 8. Hush's (1980) calculation for the Creutz–Taube complex. (a) Observed (■) and calculated intervalence band envelopes. (b) Potential energy surfaces used to calculate (a).

Mixed valency chemistry

the PKS treatment of the CT ion, namely, why has it not proved possible to observe 'tunnelling' transitions in the far infrared? From Fig. 7b one sees that in addition to the transitions between the upper and lower potential energy surfaces which give rise to the intervalence band there should exist transitions between adjacent levels in the lower surface. Since they have something of the character of an electronic charge transfer as well as a vibrational transition they ought to be much more intense than the ordinary vibrational bands, but no sign of any abnormal absorption has been seen in the CT complex at 4.2 K down to 20 cm^{-1} (Schatz *et al.*, 1978).

TYPES OF MIXED VALENCY COMPOUNDS

In the previous section some recent theoretical advances in understanding ground and excited states of mixed valency compounds have been described. In the second part of this review we shall survey experimental work on particular types of compound to exemplify the variety and vitality of the field and show how the theoretical models work out in practice.

Discrete dimers and oligomers

Evidence from structures

Following Creutz and Taube's (1969) isolation of their pyrazine-bridged Ru(II,III) ammine dimer, many other binuclear complexes $L_nM_AL_bM_BL'_n$ have been synthesized, some of which are listed in Table 3. Evidence about the classification of all these compounds comes from many different kinds of experiment. Crystal structure determinations are the most direct, but are not available in many cases. For example [(bipy)$_2$Mn(O)$_2$Mn(bipy)$_2$]$^{3+}$ (Plaksin *et al.*, 1972) has two quite distinct types of Mn coordination (Fig. 9). On the other hand there is always the possibility that small differences between the sites in an oligomer might not exceed the thermal ellipsoids in a room temperature crystal structure or, alternatively, that a molecule which almost, but not quite, has a centre of inversion or some other symmetry element, might be disordered in the crystal. Thus the CT complex, in a mixed chloride/bromide salt (Beattie *et al.*, 1977) appears to lie on such a centre (Fig. 10) though the difference between Ru(II)-N and Ru(III)-N bond lengths in the respective single valency hexammine salts is in any case no greater than 0.04 Å (Stynes and Ibers, 1971). A similar example is the trimeric complex

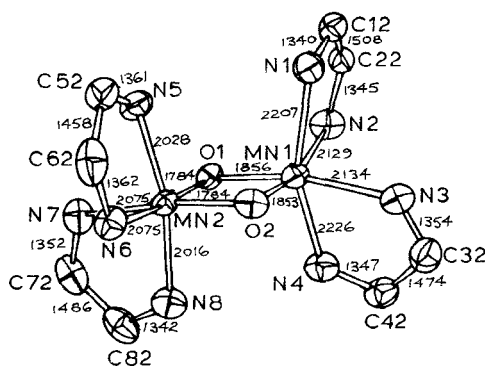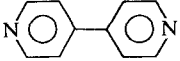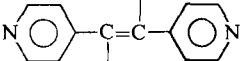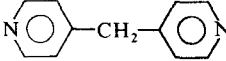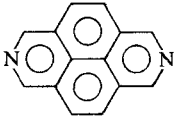FIG. 9. The molecular structure of [(bipy)$_2$MnO$_2$Mn(bipy)$_2$]$^{3+}$ (Plaksin *et al.*, 1972).

TABLE 3. Some ligand-bridged mixed valency dimeric molecules $L_nM_AL_bM_BL'_n$

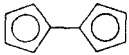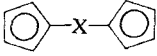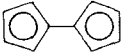|				R–D class	Ref.
Ru(II,III)	$(NH_3)_5$	$(NH_3)_5$	N◯N (pz)	II–III	a, b
			N◯—◯N (4,4' bipy)	II	c
			N◯—C=C—◯N (BPE)	II	d
			N◯—CH$_2$—◯N	II	e
			N◯◯◯N	II	d
			NC–CN	III	c
			NC–C(R)–CN	III	g
Ru(II,III)	$(bipy)_2Cl$	$(bipy)_2Cl$	pz	II	h
			4,4'-bipy	II	h
			BPE	II	h
			$Ph_2PCH_2PPh_2$	II	i
Ru(II,III)	$(NH_3)_5$	$(bipy)_2Cl$	4,4'-bipy	II	j
Os(II,III)	$(NH_3)_4Cl$	$(NH_3)_4Cl$	N_2	III	k
Fe(II,III)	$(CN)_5$	$(CN)_5$	CN	II	l
			pz,BPE	II	m
Fe(II,III)	η-C_5H_5	η-C_5H_5	◯–◯	II	n
			◯–X–◯	II	o
			(X=CH, —C=C—Hg)	I	o
Fe(II,III)	◯–◯		—	III	p
Mn(III,IV)	$(bipy)_2$	$(bipy)_2$	<O/O>	II	q

a, Creutz and Taube, 1969. b, Creutz and Taube, 1973. c, Tom *et al.*, 1974. d, Fischer *et al.*, 1976. e, Rieder and Taube, 1977. f, Tom and Taube, 1975. g, Krentzien and Taube, 1976. h, Powers *et al.*, 1976. i, Sullivan and Meyer, 1980. j, Powers *et al.*, 1976. k, Magnuson and Taube, 1972. l, Glauser *et al.*, 1973. m, Felix and Ludi, 1978. n, Morrison and Hendrickson, 1973. o, Morrison *et al.*, 1973. p, Mueller-Westerhoff and Eilbracht, 1972; LeVanda *et al.*, 1976. q, Plaksin *et al.*, 1972; Cooper and Calvin, 1977.
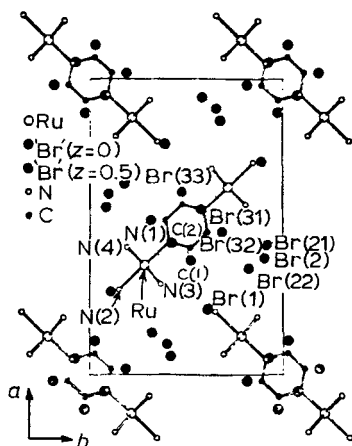
FIG. 10. The crystal structure of $[(NH_3)_5Ru(pz)Ru(NH_3)_5]Br_{10/3}Cl_{5/3}4H_2O$ (Beattie *et al.*, 1977).
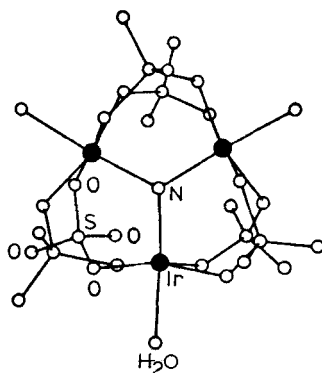
FIG. 11. The molecular structure of $[Ir_3N(SO_4)_6(H_2O)_3]^{4-}$ (Ciechanowicz *et al.*, 1971).

$[Ir_3N(SO_4)_6(H_2O)_3]^{4-}$ (Fig. 11) in which the three Ir atoms appear to have identical environments (Ciechanowicz *et al.*, 1971) although the optical and Mössbauer spectra were interpreted as consistent with a trapped Ir(III,III,IV) formulation (Brown *et al.*, 1970).

Preparation and thermodynamics

Preparation of binuclear complexes, principally by Taube, Meyer, Ludi and their coworkers, is normally accomplished by combining appropriate mononuclear complexes containing labile solvent molecules and taking advantage, where possible, of the substitution-inertness of low spin d^6 ions, for example (Meyer, 1978)

$$[Ru(bipy)_2Cl(CH_3OH)]^+ \xrightarrow[pz]{excess} [Ru(bipy)_2Cl(pz)]^+$$

$$\downarrow [Ru(bipy)_2Cl(CH_3OH)]^+ \qquad (38)$$

$$[complex]^{3+} \xleftarrow{oxidation} [(bipy)_2ClRu(pz)RuCl(bipy)_2]^{2+}.$$
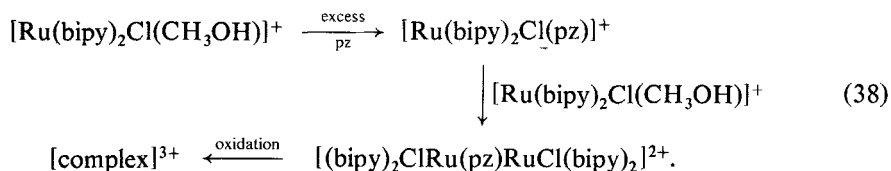
Longer chains can also be built up in this way (Powers *et al.*, 1976):

$$2[Ru(NH_3)_5(solvent)]^{2+} + [Ru(bipy)_2(pz)_2]^{2+} \rightarrow [(NH_3)_5Ru(pz)Ru(bipy)_2(pz)Ru(NH_3)_5]^{6+}. \tag{39}$$
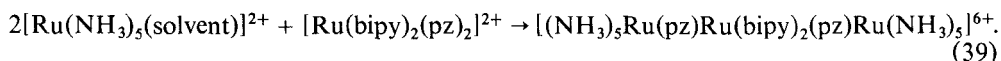
Another method would be to mix two single valence binuclear complexes, e.g. Ru(III,III) and Ru(II,II) and take advantage of a favourable conproportionation constant K_c:

$$(III,III) + (II,II) \rightleftharpoons 2(II,III). \tag{40}$$

Values of K_c are derived from the difference between the reduction potentials of the two reactions (III,III) + e → (II,III) and (II,III) + e → (II,II), the latter usually obtained by cyclic voltammetry. Measured K_c's range all the way from the statistical value for 4 for $[(CN)_5Fe(BPE)Fe(CN)_5]^{5-}$ (Felix and Ludi, 1978) through intermediate ones, e.g. 4×10^6 for the CT complex (Taube, 1978), up to 10^{20} for $[(NH_3)_5Os(N_2)Os(NH_3)_5]^{5+}$.

It is tempting to ascribe increasing values of K_c to increased interaction between the two metal ion sites, thus stabilizing the mixed valency complex, and in the case of the Os complex this is clearly true since $[(NH_3)_5Os(N_2)]^{3+}$ loses N_2 in aqueous solution at room temperature at a specific rate of 2×10^{-2} seconds (Elson *et al.*, 1970) while the mixed valency complex is produced from a solution heated at 70°C for 36 hours! Furthermore the N–N stretch in $[(NH_3)_5Os(N_2)Os(NH_3)_5]^{5+}$ is inactive in the infrared, though it appears strongly in the Raman spectrum at 1993 cm^{-1} (compare 2037 cm^{-1} in $[(NH_3)_5Os(N_2)]^{2+}$ and 2217 cm^{-1} in $[(NH_3)_5Os(N_2)]^{3+}$). Add to this the complexity of the near infrared electronic transitions which bear no resemblance to any in the Os(II) and Os(III) monomeric precursor complexes, and it seems quite clear that we have a RD class III system.

On the other hand, as Taube (1978) has pointed out, the seemingly high value of K_c for the CT complex must be interpreted with care. Consider the reduction potentials in Table 4. Adding a cation to the terminal N atom of the pyrazine renders the monomeric Ru(III) complex more oxidizing since $d \rightarrow \pi^*$ donation is enhanced in the corresponding Ru(II) state. Thus, adding CH_3 to the pyrazine increases the 3+/2+ potential from 0.49 to 0.90 V. The Ru(III),Rh(III) complex likewise has a higher potential for reduction, while the Rh(IV) → Rh(III) and Rh(III) → Rh(II) couples are respectively much more oxidizing and reducing. Note, however, that the reduction potential of the CT complex is only 0.05 V lower than that of the Ru(III), Rh(III) dimer, suggesting that stabilization of the Ru(III,II) dimer by the hole in the πd is only about 1.2 kcal. Considering also the Ru(III,II) → Ru(II,II) couple in the CT complex, the low value of 0.37 V shows that it is actually easier to extract an electron than from the monomeric Ru(II) complex, perhaps by as much as 0.2 V if the inductive effect of the other cation is taken into account. This suggests that there is some electronic factor, possibly electron repulsion arising from simultaneous delocalization of two πd electrons from opposite ends of the Ru(II,II) dimer into the pyrazine π^*-system, which is serving to destabilize the (II,II) oxidation, and that

TABLE 4. Reduction potentials of Ru(III), Ru(III,III) and Ru(II,III) complexes (Taube, 1978)

		E_f
I	$(NH_5)_5Ru(pz)^{3+/2+}$	0.49
II	$(NH_5)_5Ru(pz-CH_3)^{3+/2+}$	0.90
III	$(NH_5)_5Ru(pz)Rh(NH_5)_5^{6+/5+}$	0.79
IV	$(NH_5)_5Ru(pz)Rh(NH_5)_5^{6+/5+}$	0.74
V	$(NH_5)_5Ru(pz)Rh(NH_5)_5^{5+/4+}$	0.37

it is this effect, rather than any intrinsic stability in the (II,III) state, which accounts for the high K_c.

Nevertheless, in general smaller values of K_c correspond to weaker interaction between the two centres so that, in the limit that they behave independently, and oxidation at one end of the molecule is not correlated with oxidation of the other, the two oxidation potentials are governed only by statistical considerations. Such an evolution was observed in the cyclic voltammograms of a series of biferrocenes with different bridging groups, as in Table 5.

TABLE 5. Differences $(\Delta E_{1/2})$ between successive reduction potentials (III,III) → (III,II) and (III,II) → (II,II) of $(C_5H_5)Fe(C_5H_4)$-X-(C_5H_4)-$Fe(C_5H_5)$

X	$\Delta E_{1/2}(V)$	Ref.
$-C(CH_3)_2-C(CH_3)_2-$	0	a
$-CH=CH-$ O $CH=CH-$	0	a
$-Hg-$	0	a
$-CH_2-CH_2-$	0.04	a
$-C\equiv C-C\equiv C-$	0.10	b
$-C\equiv C-$	0.13	b
$-CH_2-$	0.17	a
directly bonded (noX)	0.33, 0.35	a, b
two direct bonds (bis-fulvalene-diiron)	0.59	a, b

a, Morrison *et al.*, 1973.
b, LeVanda *et al.*, 196

For biferrocene itself, or when the bridging group between the two cyclopentadienyl (cp) rings is conjugated, e.g. $-C\equiv C-$, two separate one-electron oxidation waves are seen, but when it is larger, e.g. $-CH_2CH_2-$, only a single wave is observed (Morrison, Krogsund and Hendrickson, 1973). Even when there is direct bonding between the two cp rings, other physical evidence such as Mössbauer (Morrison and Hendrickson, 1973) infrared and optical spectroscopy suggests that the Fe(II,III) biferrocenes remain class II, probably because the two subunits are connected in a *trans* fashion:
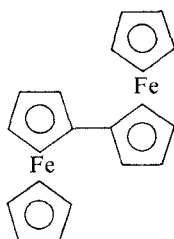
If both cp rings are fused together, though, as in the bis(fulvalene) diiron monocation, it appears that the two Fe atoms are equivalent, at least on the time-scale of Mössbauer spectroscopic transitions, i.e. the dimer is now class III, despite the fact that the Fe atoms remain separated by almost 4 Å. Clearly interaction through the π- and π^*-orbitals of the ligand must play an important role (LeVanda *et al.*, 1976).

The Creutz-Taube complex: class II or III?

Most notoriously difficult of the mixed valency dimers to classify as class II or class III has been the Creutz-Taube (CT) complex itself, for which a host of conflicting evidence and views now exists. A brief summary of the present state of knowledge is appropriate.

1. *Optical properties.* Like all Ru(II) complexes with aromatic heterocyclic ligands, the Ru(II,II) CT complex has an intense absorption in the visible assigned as a d → π^* charge transfer, which is also present in the monomeric Ru(II) pz complexes such as I and II in Table 4. As shown in Fig. 12 the band is absent from the Ru(III,III) CT complex but does appear, with roughly half the Ru(II,II) intensity, in the Ru(II,III) spectrum (Creutz and Taube, 1973). This certainly appears to support the idea that on the timescale of an optical transition (say 10^{-14} seconds) a distinct Ru(II) entity can be identified. However, the intervalence band centred at 6400 cm^{-1} (absent, of course, from the (II,II) and (III,III) complexes) is almost invariant to changes in the solvent's dielectric constant, in contrast to the bands in more weakly coupled Ru(II,III) dimers, such as those bridged by 4,4'-bipyridyl, whose energies follow Eq. (12) quite satisfactorily (Tom, Creutz and Taube, 1974). It is also worth noting that the intervalence band is quite a bit narrower than in Ru(II,III) known to be of class II type.
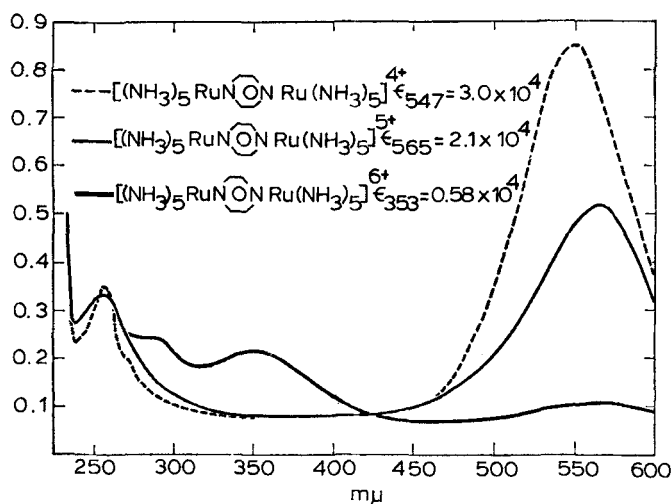
(a)
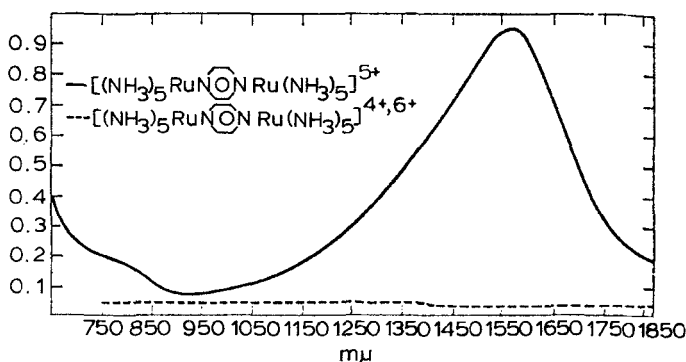
(b)

FIG. 12. Absorption spectra (a) in the visible and (b) in the near infrared of the Creutz–Taube complex (Creutz and Taube, 1969).

2. *Photoelectron spectrum.* Citrin (1973) measured the XPS spectrum of the CT complex in the Ru 3d region for all three levels of oxidation. Unfortunately the C 1s ionization from the pyrazine and organic counterion obscured part of the spectrum, which had to be 'deconvoluted'. Nevertheless the spectra of the (II,II) and (III,III) complexes each appear to consist of a doublet, due to $3d_{3/2}$ and $3d_{5/2}$ while in the (II,III) there are two doublets separated by 2 eV. Thus it appears at first sight that on this timescale (10^{-16} seconds) individual oxidation states can be distinguished. Quite recently Citrin and Ginsberg (1981) remeasured the XPS spectra, extending the data to the Ru 3p peaks, which are not covered by ionization peaks from other elements, and also taking particular care to avoid radiation damage. They confirm that there are indeed two sets of core level ionization peaks in the (II,III) complex, with equal intensities and with binding energies close to those in the (II,II) and (III,III). A naïve interpretation of these facts is that the CT complex is class II, but a further subtlety must be remarked.

Hush (1975) has argued that two sets of ionization peaks might still be observed even if there were complete charge delocalization. Upon creation of a core hole by photoionization the valence shell orbital relaxes strongly, even if originally delocalized, and the system becomes localized. Then there are two final states of photoionization, a lower one having the valence electron localized on the same centre as the core hole and one of higher energy in which the valence electron is on the other centre. In Hush's treatment the intensities of the two peaks depend on the extent to which the charge is localized and the observed ratio of 1.0 would indicate localization. However, Citrin and Ginsberg (1981) note that the electronic coupling integral, V_{01} (or ε in the PKS model) is bound to be different in the photoionized state than in the ground state. If, as is likely, it is much smaller then it turns out that the ratio of the intensities of the two photoionization peaks should be 1.0 irrespective of whether the complex is class II or III, i.e. core-shell photoelectron spectroscopy cannot be used to distinguish the extent of the localization or delocalization in the valence shell. It is interesting to note that the idea of localization by core hole polarization in a photoionized state was suggest by Friedel (1969) for metals and has also been used to account for splittings in the XPS of metallic (i.e. indubitably class III) tungsten bronzes (Chazalviel *et al.*, 1977).

3. *Vibrational spectra.* The first infrared spectra of the CT complex were measured on the tosylate salt (Creutz and Taube, 1973) and there was some difficulty in disentangling parts of the spectrum of the cation from that of the anion. Some indication was found, however, that the symmetric NH_3 rocking frequency in the (II,III) complex was intermediate between (II,II) and (III,III) rather than a superposition of the two. Later measurements by Beattie, Hush and Taylor (1976) on the bromide salt confirmed that the rocking mode was at 800 cm^{-1} in the (II,III) ion compared with 750 and 840 cm^{-1} in (II,II) and (III,III), and a further Ru–NH_3 band at 449, compared with 438 and 461 cm^{-1}. Similarly, a band attributed to an Ru–pz stretching mode was at 316 cm^{-1} compared with 310 and 320 in the two single valence ions, though in this case the energy difference between the bands is not much greater than their halfwidths. Thus there appears to be some evidence that the CT complex is delocalized on the timescale 10^{-12}–10^{-13} seconds. However, it has been claimed (Strekas and Spiro, 1976) that irradiating into the visible electronic absorption band, assigned above to Ru(II)d → pzπ^* charge transfer, causes resonance enhancement of a Raman transition corresponding to an Ru(II)–pz stretching mode. Further experiments of this kind would be most welcome.

4. *Mössbauer spectrum.* In principle one could use the Mössbauer spectrum to distinguish whether the electron transfer rate (given, for example, by Eq. (9)) is greater or less than the nuclear excited state decay time for the element in question. Clear-cut instances of both extremes are found among Fe(II,III) compounds—$Fe_2F_5 7H_2O$ is class I (Walton *et al.*, 1976) and bis(fulvalene)diiron monocation (Morrison and Hendrickson, 1973) is class III

for example—but application of the technique to the CT complex has been less than satisfying. ^{99}Ru has only a low recoilless fraction above 4.2 K so spectra can only be recorded at that temperature. Furthermore the only published spectrum of the CT complex was obtained with a very small sample (Creutz, Good and Chandra, 1973), and consequently poor statistics. Nevertheless it proved possible to fit it to a convolution of three peaks, one assigned to low-spin Ru(II) with a $^1A_1$ ground state and the other pair to Ru(III), split by the quadrupole interaction in the $I = 3/2$ nuclear excited state. It would be very desirable to repeat these measurements to improve the signal-to-noise ratio, but even so, there seems little doubt that a class II ground state has been observed at 4.2 K.

5. *Magnetic susceptibility.* No data are available for the (II,III) ion but the moment of the (III,III) dimer varies with temperature from 300 down to 15 K in a manner which parallels that of $Ru(NH_3)_6Cl_3$ (Bunker *et al.*, 1978). This has been taken as evidence, first that the oxidized dimer contains two unpaired electrons of essentially Ru 4d type and, second, that there is only a very weak interaction between them. The moment of the dimer falls very rapidly below 15 K but it is not known whether this is due to intramolecular or inter-molecular antiferromagnetic coupling. In either case the argument is that since the unpaired spins in the (III,III) complex scarcely interact, it would be remarkable if the single unpaired spin in the (II,III) dimer were delocalized between the two metal atoms.

6. *Paramagnetic resonance.* The first e.p.r. measurements on the CT complex to be published were those of Bunker *et al.* (1978) who used frozen solutions in Me_2SO: glycerol at 24 K. They found that the (III,III) dimer had $g_\perp = 2.68$, almost the same as that of a Ru(III) pz monomeric complex and also Ru(ethylenediamine)$_3^{3+}$ which had been measured earlier in a single crystal. The four NH_3 ligands around each Ru in the CT complex lie at 45° to the pyrazine plane so with X as the Ru–Ru axis, Z normal to the pz plane and Y within the plane the relevant one-electron orbitals are

$$|a\rangle = (1/\sqrt{2})(|z^2 - y^2\rangle + i|xy\rangle)$$
$$|b\rangle = (1/\sqrt{2})(|z^2 - y^2\rangle - i|xy\rangle). \tag{41}$$

Expressions relating the observed g-values to the splitting of an octahedral $^2T_{2g}$ ground term by tetragonal distortion and spin-orbit coupling were given by Stevens (1953) in the form

$$g_{\parallel} = 2 \,|\, (1 + k)\cos^2\alpha - \sin^2\alpha \,|$$
$$g_{\perp} = 2 \,|\, \sqrt{2}k\cos\alpha\sin\alpha + \sin^2\alpha \,| \tag{42}$$

where $\tan 2\alpha = \sqrt{2}(\tfrac{1}{2} - t/\zeta)^{-1}$. The parameter t is the energy difference between the $^2B_{2g}$ and ^2E_g components of $^2T_{2g}$ in the tetragonal field, ζ is the spin-orbit coupling constant, equal to -1050 cm^{-1} and k is the orbital reduction factor. The predicted variation of $g_{\parallel}$ and $g_{\perp}$ with t/ζ is shown in Fig. 13 for $k = 1.0$ and 0.96. The measured $g_{\perp}$ was 2.68. Bunker *et al.* could not observe $g_{\parallel}$ and therefore they assumed that it was very low, corresponding to $t/\zeta \sim 1$, a value consistent with a localized ground state having $g_{\parallel}$ aligned parallel to the X (Ru–Ru) axis, along which the crystal structure demonstrates that there is indeed an axial compression. Quite recently, however, Hush, Edgar and Beattie (1980) re-examined the e.p.r. spectrum of the CT complex using a single crystal instead of a frozen solution. They confirmed $g_{\perp} = 2.632 \pm 0.005$ but in addition found $g_{\parallel} = 1.334 \pm 0.010$. From Fig. 13 these values would define $t/\zeta \sim 2.3$. Furthermore the $g_{\parallel}$ component is actually aligned along the Z axis, i.e. perpendicular to the plane of the pz and to the Ru–Ru axis. Hush *et al.* (1980) note that this is exactly what would be expected if the electronic structure were dominated by strong dπ–pπ bonding, and is hence quite compatible with a delocalized ground state. What is not clear, however, is that the result is definitely incompatible with a weakly delocalized state.
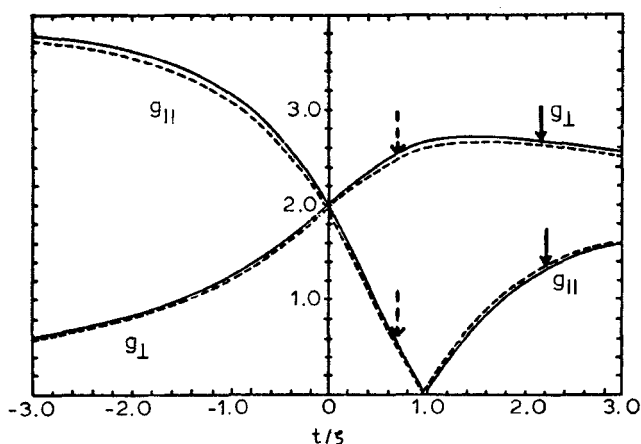
FIG. 13. Calculated $g_\parallel$ and $g_\perp$ for the Creutz–Taube complex as a function of t/ζ. (———) orbital reduction factor $k = 1.0$ and (– – – –) for $k = 0.96$. (←– –→) indicate g-values from Bunker *et al.* (1978) and (———→) from Hush *et al.*, 1980.
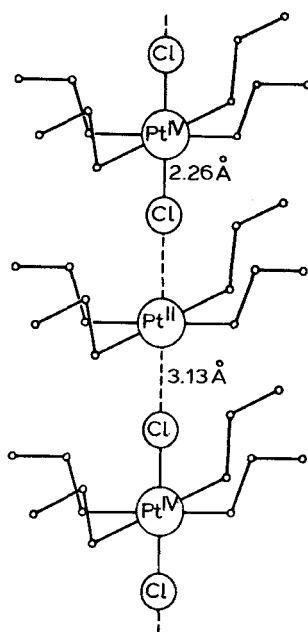
FIG. 14. The structure of Wolfram's Red Salt (Craven and Hall, 1961).

7. *Nuclear magnetic resonance.* Methanol-Me$_2$SO solutions of the CT complex in all three states of oxidation show a single broad resonance due to the p protons, that in the (II,III) ion being intermediate both in chemical shift and linewidth between those of the two single valency ions (Bunker *et al.*, 1978). Consequently the (II,III) is delocalized on the n.m.r. timescale (say 10^{-6} seconds) at $-80°$C.

We have gone into considerable detail about the evidence obtained from a wide range of physical methods about the extent of electron delocalization in the CT complex because,

TABLE 6. Estimates of the ground state of the Creutz-Taube complex
$[(NH_3)_5Ru(pz)Ru(NH_3)_5]^{5+}$ by various experimental methods

	Timescale (seconds)		Ref.
Core-shell photoionization	10^{-16}	Uncertain	a
Pz π-π^* and Ru d $\rightarrow \pi^*$ absorption	10^{-14}	Localized	b
Intervalence transition	10^{-13}		
Solvent dependence		Delocalized	c
Bandshape		Borderline, delocalized	d
Infrared spectrum	10^{-12}	Uncertain, probably localized	e
Resonance Raman spectrum	10^{-12}	Localized	f
Paramagnetic resonance	10^{-9}	Uncertain, probably delocalized	g
NMR	10^{-7}	Delocalized	h
Mössbauer spectroscopy	10^{-6}	Localized	i
Crystal structure		Delocalized	j

a, Citrin, 1973; Hush, 1975; Citrin and Ginsberg, 1981. b, Creutz and
Taube, 1969; Mayoh and Day, 1972, 1974. c, Creutz and Taube, 1973. d,
Piepho *et al.*, 1978; Beattie *et al.*, 1976. e, Creutz and Taube, 1973; Beattie
et al., 1976. f, Strekas and Spiro, 1976. g, Bunker *et al.*, 1978; Hush *et al.*,
1980. h, Bunker *et al.*, 1978. i, Creutz *et al.*, 1973. j, Beattie *et al.*, 1977.

in the minds of many workers in the field, it has evidently taken on the character of a
paradigm case. Some of the lines of evidence certainly conflict, partly because of the
enormous range of timescales they encompass but partly, too, because of problems about
the detailed interpretation of the experiments themselves (e.g. XPS and e.p.r.). Table 6
attempts a summary of the conclusions now current concerning the nature of the CT ion,
together with the timescales sampled by the various techniques. The best that can be said
at present is that the electron transfer rate is certainly greater than 10^5 seconds^{-1} and
probably greater than 10^{12} seconds^{-1}. It must be emphasized very forcibly, though, that
the very existence of such a conflict of evidence as we have described means that the CT
complex certainly lies near the borderline between classes II and III and thus is very far
from being a typical case. In almost all other dimeric or oligomeric mixed valency
complexes the various strands of evidence agree quite firmly on localization over the
longest timescales available experimentally, or delocalization over the shortest. Indeed,
given the very large number of mixed valency complexes whose properties have now been
studied it is quite remarkable how few have electron transfer rates lying within the range
spanned by the various spectroscopic methods. Interesting recent exceptions to this
generalization are the temperature dependent Mössbauer spectra of the trinuclear basic
acetate $Fe(II)Fe(III)_2O(CH_3COO)_6(H_2O)$ (Dziobkowski, Wrobleski and Brown, 1981)
and the temperature dependent e.p.r. of the Mo(V,VI) heteropolyblue anion $Mo_6O_{19}^{3-}$
(Che, Fournier and Launay, 1979), in both of which one finds evidence for rapid electron
hopping at room temperature, but localization on to a single site at 77 K.

One-dimensional complexes

After discrete dimeric or oligomeric molecules, the infinite lattice systems containing
interacting mixed valency metal ions which might be expected to be the easiest to under-
stand in detail are those in which the interactions extend only in one dimension, i.e.

linear chain compounds. Very many inorganic and metal-organic compounds form lattices containing chains of closely-spaced metal ions, and their physical properties cover the whole gamut from insulators containing essentially non-interacting metal ions, through substances with appreciable magnetic exchange interactions all the way to the now famous one-dimensional metallic conductors. It is the peculiar properties of the latter which has focused so much attention on one-dimensional mixed valency compounds. I have drawn attention to correlations between structure and physical properties in both single and mixed valency metal chain compounds in other articles (Day, 1974, 1975, 1977, 1978), and will not repeat the discussion here. Suffice it to say, in the present context, that there are two major categories of mixed valency metal chain complexes, namely those in which the metal atoms along the chain alternate with bridging anions, and those in which the chain is composed solely of metal atoms. Evidence to be briefly summarized here leads to the conclusion that all the former are of class II type while all the latter belong to class III.

Class II complexes with bridging anions: Wolfram's Red Salt

The prototype mixed valency chain compound with anion bridging groups is Wolfram's Red Salt, $[Pt(C_2H_5NH_2)_4][Pt(C_2H_5NH_2)_4Cl_2]Cl_4$ $4H_2O$, (WRS) whose structure is shown in Fig. 14. Like so many of the mixed valency compounds first prepared in the last century, its trivial name emphasizes its colour, which is in striking contrast to the colours of its two constituent complexes of Pt(II) and Pt(IV). In all the compounds of this kind the dominant structural motif is a square of ligands around each Pt, with its plane perpendicular to the axis of the chain. The ligands may be NH_3, RNH_2 (R = alkyl), $H_2N(CH_2)_2NH_2$ or halide ions as in $Pt(NH_3)_2Cl_3$. In every case however, the stacking of these planar units is accomplished via halide ion bridges, so that the 'operative' part of the linear structure consists of a diatomic chain. However, the feature of greatest importance in determining the electronic behaviour of the chain is that the chain is not uniform, but dimerized. The Pt—X distances alternate so as to produce two distinct Pt sites, one with four planar ligands and two axial halide ions much more distant, the other also with four planar ligands but now with the two axial halide ions much closer. Table 7 collects structural data about some of these compounds. Although there is some variation within each set with the counter-ion or equatorial ligands, there is a clear trend towards equalizing the Pt—X and Pt $\cdots$ X bond lengths as one passes from Cl to Br to I (average values of p are 0.72 ± 0.10 for Cl, 0.82 ± 0.14 for Br and 0.93 ± 0.02 for I). Nevertheless, in all compounds of the WRS type the two Pt sites are clearly distinguishable, so class II mixed valency behaviour is to be expected. Briefly we now survey the evidence from physical properties.

1. *Photoelectron spectroscopy.* Burroughs *et al.* (1975) made a very careful study of $(Pt(en)Cl_2)(Pt(en)Cl_4)$ (en = ethylenediamine) in the Pt 4f region. They found that the spectrum consisted of three peaks (Fig. 15) which, however, could be deconvoluted into two pairs arising from 4f(5/2) and 4f(7/2) spin-orbit components from Pt(II) and Pt(IV). In Fig. 15 we also reproduce the 4f region of $Pt(en)Cl_4$, showing the single pair of spin-orbit components from Pt(IV). Interpretation of the XPS of this type of compound is not quite so straightforward as it may appear because, as is well known, the technique is extremely sensitive to surface impurities and mixed-valency compounds especially are liable to oxidize or reduce superficially, either in the atmosphere or under X-ray bombardment. Indeed, starting with $Pt(en)Cl_4$, Burroughs *et al.* were able to demonstrate that increasing exposure to the Al $K\alpha$ exciting radiation produced XPS signals first of $Pt(en)Cl_4$, then of the mixed valency compound $(Pt(en)Cl_2)(Pt(en)Cl_4)$ and finally of

TABLE 7. Structural data on compounds of the Wolfram's Red Salt (WRS) type

Axial bridging ligand	Equatorial ligand(s)	Counter-ion	Pt–X(Å)[a]	Pt···X(Å)[a]	Pt–Pt[b]	ρ[c]	Ref.
Cl	$C_2H_5NH_2$	Cl,H_2O	2.26	3.13	5.39	0.72	d
Cl	$H_2N(CH_2)_3NH_2$	BF_4	2.30	3.10	5.40	0.74	e
Cl	$H_2N(CH_2)_2NH_2$	$CuCl_4$	2.33	2.93	5.26	0.79	f
Cl	NH_3,Cl	—	2.03	3.30	5.33	0.61	g
Br	$C_2H_5NH_2$	Br	2.28, 2.68	3.41, 3.81	6.09	0.69	h
Br	$C_2H_5NH_2$	Br,H_2O	2.45, 2.48	3.11, 3.14	5.59	0.79	i
Br	$H_2N(CH_2)_2NH_2$	ClO_4	2.71	2.76	5.47	0.98	j
Br	$H_2N(CH_2)_3NH_2$	ClO_4	2.55	2.96	5.51	0.86	e
Br	$H_2NCH(CH_3)CH_2NH_2$	Cu_3Br_5	2.55	3.07	5.62	0.83	k
Br	NH_3,Br	—	2.50	3.03	5.53	0.83	l
Br	$H_2N(CH_2)_2NH_2$,Br	—	2.48	3.12	5.60	0.79	m
I	I	K	2.74	3.00	5.74	0.91	n
I	$H_2N(CH_2)_2NH_2$	ClO_4	2.79	3.04	5.83	0.92	o
I	$H_2NCH(CH_3)CH_2NH_2$	ClO_4	2.77	2.96	5.73	0.93	p
I	$H_2NCH(CH_3)CH_2NH_2$	I	2.81	2.99	5.80	0.94	j

a, Short and long Pt–halide distances along the chain. b, closest Pt–Pt distance along the chain. c, (Pt–X)/ (Pt···X). d, Craven and Hall, 1961. e, Matsumoto et al., 1978. f, Endres et al., 1979. g. Wallen et al., 1962. h, Endres et al., 1980. i, Brown and Hall, 1976. j, Endres et al., 1980. k, Keller et al., 1978. l, Hall and Williams, 1958. m, Ryan and Rundle, 1961. n, Thiele, 1977. o, Endres et al., 1980. p, Breer et al., 1978.
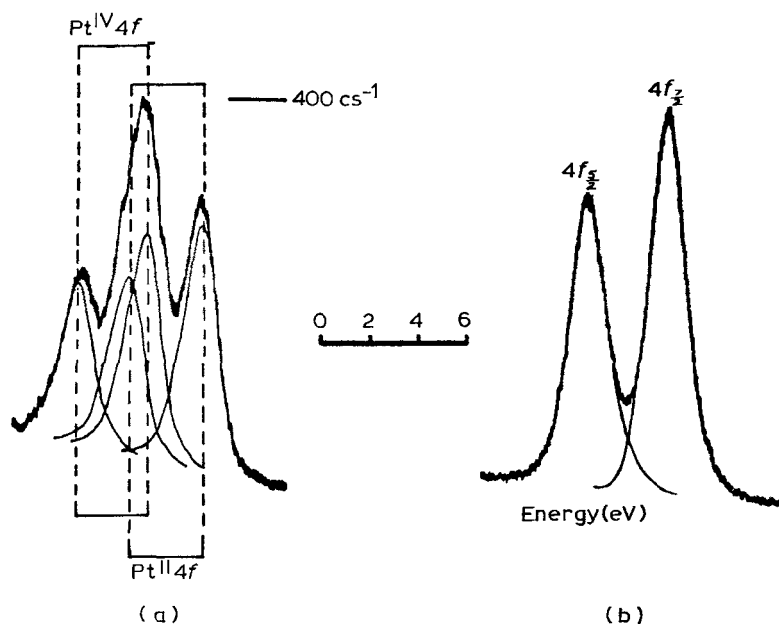
FIG. 15. XPS of (a) [Pt(en)Cl$_2$||Pt(en)Cl$_4$], (b) Pt(en)Cl$_2$ in the Pt 4f region (Burroughs et al., 1975).

Pt(en)Cl$_2$. Such radiation-induced reactions at the surface are quite common, and constitute a hazard to interpreting the XPS of many other mixed valency compounds. Examples which have been investigated quite thoroughly in this way include Cs_2SbCl_6 (Tricker et al., 1972, Burroughs et al., 1974) and Sb_2O_4 (Orchard and Thornton 1977). Nevertheless, it seems quite clear that all the WRS group of compounds have separate

XPS signals from Pt(II) and Pt(IV), though it has been claimed by Yamashita *et al.* (1978) that the difference in 4f bridging energy at the two sites decreases as the bridging anion is changed from Cl to Br to I, following the diminished difference between the Pt–X and Pt $\cdots$ X bond lengths.

2. *Optical spectroscopy.* The red colour of WRS (and the green colour of Reihlen's Green Salt, its bromide analogue!) has its origin in an extremely intense absorption band covering most of the visible region of the spectrum. Because the absorption is so strong the transmission spectra of single crystals of these compounds are very hard to measure. The early work of Yamada and Tsuchida (1956) in this field is marred by stray light, which entered their spectrometer and obscured the upper parts of the absorption bands. More recently it proved possible to record the polarized transmission spectrum of a microscopic single crystal of WRS (Fig. 16) using condensing optics and cooling the crystal in a helium gas flow tube (Crabtree, 1972). The absorption in the visible is almost entirely confined to the spectrum recorded with the electric vector parallel to the metal chains, with the exception of the small band at 3900 Å, assigned as the first ligand field transition of the $[Pt(C_2H_5NH_2)_4Cl_2]^{2+}$ moiety. The intense absorption with E//c appears composite (a point of some importance in interpreting the resonance Raman enhancement profiles, see below) but it does not seem to be an artifact resulting from stray light or incomplete polarization. The most convenient way to derive the optical properties of highly absorbing materials is to measure normal-incidence reflectivity spectra, a technique which has been applied to salts of the WRS type by Breer *et al.* (1978) and Papavassiliou and Zdetsis (1980). One such spectrum is shown in Fig. 17. With the electric vector of the incident light perpendicular to the chain axis the reflectivity is low and constant throughout the visible and near infrared but when it is parallel to the chain axis there is a broad peak. The reflectivity can be written (e.g. Anex and Simpson, 1960) in terms of the complex dielectric constant ε as

$$R = \frac{1 + |\varepsilon| - [2(|\varepsilon| + \varepsilon_1)]^{1/2}}{1 + |\varepsilon| + [2(|\varepsilon| + \varepsilon_1)]^{1/2}} \tag{43}$$

where ε_1 and ε_2 are the real and imaginary parts of ε, i.e.

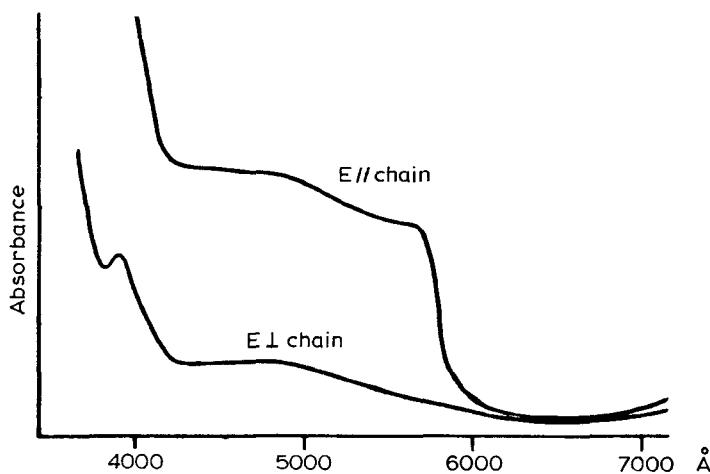$$|\varepsilon| = (\varepsilon_1^2 + \varepsilon_2^2)^{1/2}. \tag{44}$$

FIG. 16. Polarized absorption spectrum of Wolfram's Red Salt at 4.2 K (Crabtree, 1972).
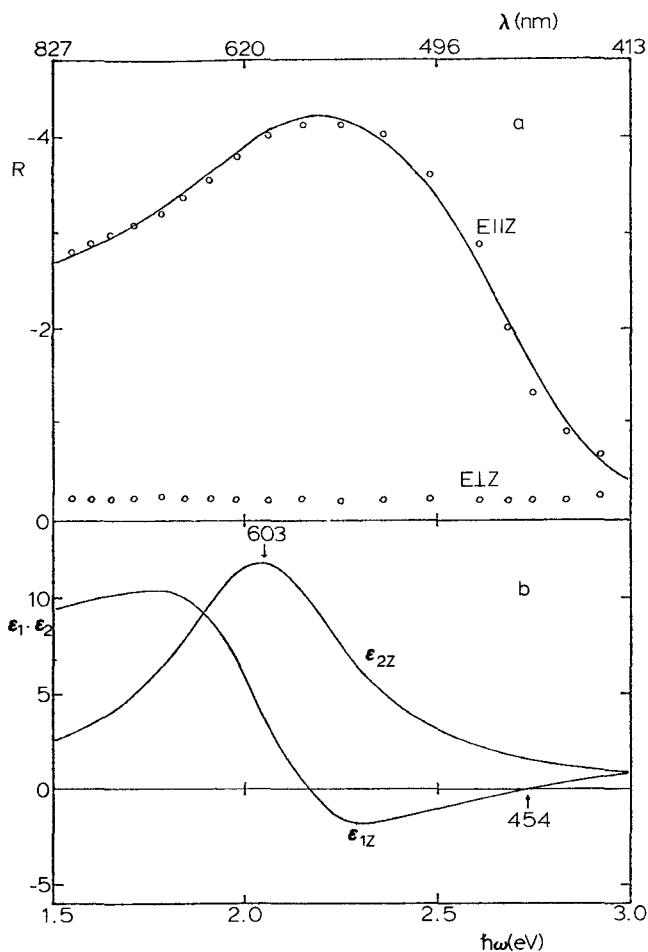
FIG. 17. (a) Polarized reflectivity of $[Pt(dapn)_2Pt(dapn)_2Br_2](ClO_4)_4$. The circles are experimental points and the full line calculated with the parameters listed in Table 8. (b) Calculated frequency dependence of ε_1 and ε_2 (Papavassiliou and Zdetsis, 1980).

It is customary to assume that the frequency dependence of ε obeys a damped Lorentzian function:

$$\varepsilon(\omega) = \varepsilon(\infty) + \frac{\omega_p^2}{\omega_g^2 - \omega^2 - (i\omega/\tau)} \qquad (45)$$

where ω_p is the plasma frequency, given by $\omega_p^2 = 4\pi N_0 e^2/m$ (N_0 is the effective electron density and in the effective electron lines), ω_g is the gap frequency and τ is a damping factor, essentially the electronic relaxation time. Pappavassiliou and Zdetsis (1980) used a least-squares procedure to fit the observed reflectivity to Eqs. (43) and (45) so as to derive the optical constants. Their results for $[Pt(dapn)_2Pt(dapn)_2Br_2](ClO_4)_4$ are shown in Fig. 17b and the full line in Fig. 17a shows the quality of the fit. In Table 8 we give the optical parameters for all three members of this series.

TABLE 8. Optical parameters of the linear chain mixed valency compounds $[Pt(dapn)_2Pt(dapn)_2X_2]$-$(ClO_4)_4$ (dapn = 1,2 diaminopropane) (Pappa-vassiliou and Zdetsis, 1980)

X	$\varepsilon(\infty)$	$\varepsilon(0)$	$\hbar\omega_g$ (eV)	$\tau(10^{-15}$ s)
Cl	1.62	2.60	2.61	3.20
Br	3.55	6.81	2.06	1.77
I	1.99	9.07	1.13	1.89

Most striking among the data in Table 8 is the strong dependence of the gap frequency on the bridging halide ion. Given that in their other physical and structural properties the WRS salts are typical class II compounds the excited states listed in Table 8 should be assigned as intervalence transitions, Pt(II) → Pt(IV). There has been a lot of discussion since the mid-1960s about the relative ordering of the 5d-based valence shell orbitals in square planar d^8 complexes (e.g. Day *et al.*, 1965; Martin, 1971) but there is now a good consensus that in most cases where strong σ- and π-donor ligands are concerned, the order is as shown on the left hand side of Fig. 18. It is important to notice that both the Pt(II) and Pt(IV) sites in the WRS compounds have D_{4h} point symmetry, and the relative valence shell orbital ordering in a tetragonally distorted six-coordinate Pt(IV) complex is shown on the right hand side of Fig. 18. Appropriate donor and acceptor orbitals for the electron transfer between Pt(II) and Pt(IV) are the respectively filled and empty z^2 orbitals. Note, however, that the Pt–Pt distance along the chain (Table 7) is between 5 and 6 Å, so direct overlap between these orbitals is negligible. Just as in the Ru(II,III) dimers (page 166) we must invoke participation of orbitals on the bridging ligands, most appropriately through the perturbation model for bridging ligands (page 154). The 'local' charge transfer excited states which provide the intervalence interaction in that model certainly fall in energy in the order Cl > Br > I, and it may be significant that the intervalence transition energies themselves in the $[Pt(dapn)_2Pt(dapn)_2X_2](ClO_4)_4$ salts (Table 8) decrease by nearly the same amount from X = Cl to Br and X = Br to I as the X → M charge transfer transitions in transition metal halide complexes (e.g. Jørgensen, 1970).
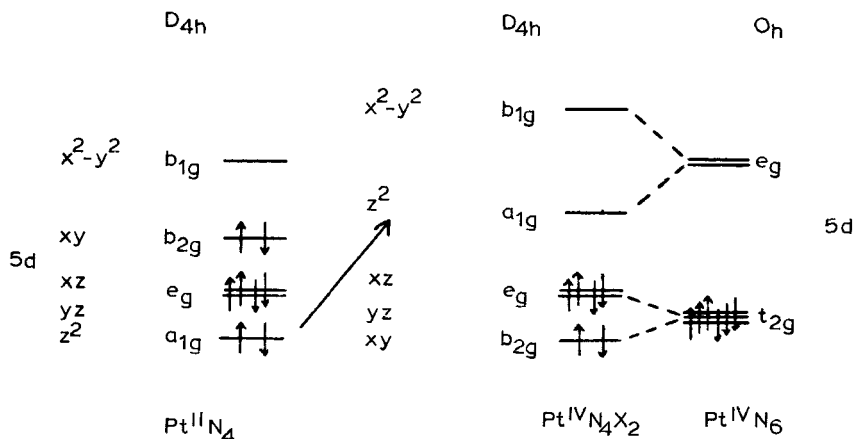

FIG. 18. Ligand field levels of Pt(II) and Pt(IV) in Wolfram's Red Salt. The postulated intervalence transfer is arrowed.

Nevertheless, two points about the intervalence transitions in one-dimensional Pt(II,IV) compounds must be borne in mind. First, the lattices *are* one-dimensional, i.e. they contain infinite chains of metal atoms. Consequently the intervalence states must be treated, strictly speaking, as excitons. Thus, if the ground state of the chain is written as

$$\phi_0 = \varphi_1^{II} \varphi_2^{IV} \varphi_3^{II} \cdots \varphi_{2N-1}^{II} \varphi_{2N}^{IV} \tag{46}$$

where the φ are 5d z^2-based molecular orbitals on the alternating Pt(II) and Pt(IV) centres, a single site intervalence excited state wavefunction would be

$$\phi_n = \varphi_1^{II} \varphi_2^{IV} \cdots \varphi_n^{III} \varphi_{n+1}^{III} \cdots \varphi_{2N-1}^{II} \varphi_{2N}^{IV} \tag{47}$$

and the exciton wavefunction

$$\phi_n(\mathbf{k}) = N^{-1/2} \sum \exp(i\mathbf{k}\mathbf{r}_n) \, \phi_n. \tag{48}$$

Since transfer of an electron from φ_n^{II} to φ_{n-1}^{IV} is completely equivalent to transfer to φ_{n+1}^{IV} the exciton wavefunction is a linear combination of the two, so for $\mathbf{k} = 0$

$$\psi_{\pm n}(0) = 2^{-1/2}[\phi_{n+1}(0) \pm \phi_{n-1}(0)]. \tag{49}$$

From the local symmetry one can see that only the transition to $\psi_{-n}(0)$ would be electric-dipole-allowed. The second point which distinguishes these excited states from, e.g. the Ru(II,III) ones, is that the oxidation states of the two metal ions in the ground states differ by two units instead of one. Pairs of potential energy surfaces of the type shown in Fig. 3 are not appropriate, therefore, and have to be replaced by a set of three surfaces as in Fig. 19. Those labelled (II,IV) and (IV,II), in an obvious nomenclature, are orthogonal since they differ by two electrons but either can interact with (III,III), whose minimum lies symmetrically between the other two in the configuration coordinate diagram, but at an unknown energy above them. The same kind of diagram would be needed, of course, to rationalize the optical spectra of other mixed valency compounds in which the oxidation states differ by two units, e.g. Sb(III,V) (page 158).

3. *Vibrational spectra.* The infrared and normal Raman spectra of the WRS compounds are precisely what one would expect of class II mixed valency, namely, vibrational transitions close to being a superposition of those of the Pt(II) and Pt(IV) complexes making up the chains. What is really exceptional and remarkable, however, is the appearance of the resonance Raman spectra excited at frequencies lying inside the intervalence absorption band envelope. A typical example is shown in Fig. 20. The spectrum, which only appears with such enhancement when the electric vector of the exciting light is parallel to the chain, is dominated by a very long progression (up to 18 members) in one
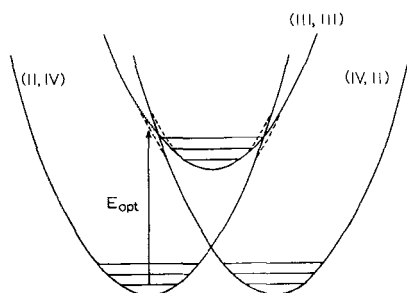

FIG. 19. Potential energy surfaces for Wolfram's Red Salt. The dashed lines indicate regions of 'non-crossing'.
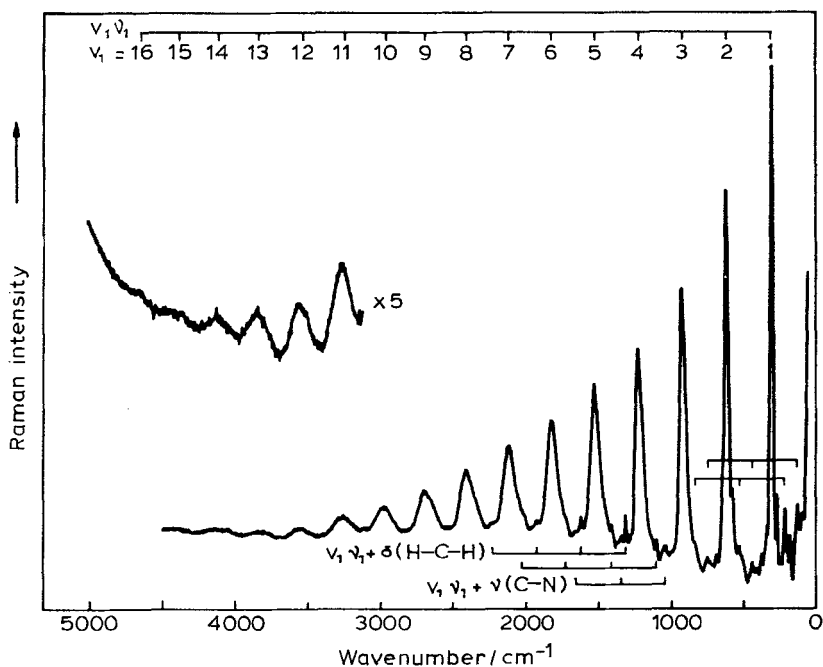
Mixed valency chemistry

FIG. 20. Resonance Raman spectrum of Wolfram's Red Salt at 80 K (Clark, 1978).

single mode, namely the axial v_1 X–Pt–X symmetric stretching mode. Clark (1977, 1980) and Pappavassiliou, Layek and Theophanides, (1980) have measured many spectra of this kind which, from the theory of the resonance Raman effect, betoken a very large displacement of the electronically excited state along this particular vibrational coordinate. Of course, this is exactly what one would expect if the excitation is to an intervalence state such as that of Eq. (47) because its relaxed configuration (Fig. 19) would have the axial bridging halide ion midway between the two Pt(III) ions.

Mingardi and Siebrand (1975) showed how to estimate how much the excited state is displaced along the v_1 vibrational coordinate by measuring the intensities $I_{0(n+1)}/I_{0n}$ of successive resonance Raman lines in the progression. Application of their theory to the WRS compounds is most instructive. Labelling the minimum energies of the ground and excited state potential energy surfaces as E_{00} and E_{10} (as in Fig. 3) the equations of the two surfaces are

$$E_0(q) = E_{00} + (1/2)\,\mu_0\,\omega_0^2 q^2$$
$$E_1(q) = E_{10} + (1/2)\,\mu_1\,\omega_1^2(q - q_1)^2 \tag{50}$$

where the μs are reduced masses, the ωs are the vibrational frequencies in the two states and we assume that E_{00} lies at $q = 0$ while E_{10} is displaced by q_1 along the vibrational coordinate concerned. With these definitions Mingardi and Siebrand (1975) show that

$$(I_{02}/I_{01})^2 \sim g\gamma(0.61\,g^2 + \gamma)^{-2} \tag{51}$$

where

$$g = (E_{opt} - E_{inc} - i\Gamma)/\hbar\omega_1$$
$$\gamma = (1/2)\,\mu_1\,\omega_1^2 q_1^2/\hbar\omega. \tag{52}$$

In Eq. (52) E_{opt} is the energy of the Franck–Condon maximum of the intervalence band, as in Fig. 3, while E_{inc} is the energy of the exciting radiation, and Γ is a damping function describing the widths of the individual vibronic lines. Of course, such lines are never observed in intervalence transitions, as we pointed out, so Γ must be estimated. Nevertheless, combining the observed values of E_{opt} (21 000 cm^{-1}) and ω (319.5 cm^{-1}) for WRS at room temperature, with I_{02}/I_{01} of 0.55 at an excitation frequency of 19 436 cm^{-1} (Clark, Franks and Trumble, 1976) one finds that $q_1 \sim 0.50$ Å. This estimate should be compared with the difference of 0.87 Å between the Pt(II)–Cl and Pt(IV)–Cl bond lengths in WRS at room temperature, and serves to show that they are indeed almost equalized in the relaxed intervalence excited state. At low temperatures (80 K, Clark, 1980) the ratios I_{02}/I_{01} become even larger, but we have no information on the bond lengths under these conditions.

The theory of Mingardi and Siebrand (1975) was designed to deal with the electronic and vibrational states of molecules, but just as we wrote the wavefunctions of the electronic excited states of the infinite mixed valency chains as Frenkel excitons (Eq. (48)) so it is also strictly correct to write those of the vibrational states as phonons rather than individual X–Pt–X modes. The classical problem of the vibrational modes of a dimerized diatomic chain was solved recently by Paraskevaidis and Papatriantafillou (1980), and should form the basis for the correct solid state solution of the resonance Raman effect in these compounds, taking account of the interactions of the excitons and phonons, much as in continuous lattice semiconductors such as CdS. Such a programme has not yet been carried out, but may provide the answer to a puzzling feature of the resonance Raman spectra, namely, that their excitation profiles do not follow the intervalence absorption profile, at least as measured by powder diffuse reflectance spectroscopy (Fig. 21). On the other hand it may simply be that the excitation profile is following the profile of the imaginary part of the refractive index (compare the excitation profile of Reihlen's Green Salt in Fig. 21 with the ε_2 curve of a similar bromide salt in Fig. 17b.

4. *Electrical conductivity.* Corresponding to adiabatic electron transfer in the dimeric Ru(II,III) complexes described earlier, electron transfer along an infinite chain might be detectable as electrical conductivity. Given their highly anisotropic structures, it is no surprise that the conductivity of crystals of WRS type is much larger parallel than perpendicular to the chains. For example $\sigma_\parallel/\sigma_\perp \sim 300$ was reported for [Pd(NH$_3$)$_2$Cl$_2$]-[Pd(NH$_3$)$_2$Cl$_4$] by Thomas and Underhill (1969, 1971) but the absolute specific conductivity $\sigma_\parallel$ was low (3 × 10^{-9} Ω^{-1} cm^{-1} at room temperature), as anticipated for a class II compound. With pressure, however, the conductivity rises dramatically, and at 130 kbar has reached 0.2 Ω^{-1} cm^{-1} (Interrante, Browall and Bundy, 1974). Most likely, the increase in conductivity with pressure comes about because the Pt(II)–X and Pt(IV)$\cdots$X bond lengths move closer to equivalence, so reducing (E_1-E_0) in Fig. 3. No information has been published about the structures of WRS crystals at high pressure, but it is worth pointing out that in another halide-bridged mixed valency chain compound Cs$_2$[AuCl$_4$]-[AuCl$_2$] (Well's Salt) there is definite evidence for a shift in the Au(I)–Cl and Au(III)–Cl bond lengths with pressure (Day, Vettier and Parisot, 1978), so that at 60 kbar they become equal (Denner, Schulz and d'Amour, 1978) and the substance is then a metal (Keller, Fenner and Holzapfel, 1974).

Class III chains with directly interacting metal atoms: KCP

In the mixed valency metal chains with halide bridging groups, the halide bridges cause the valence trapping, and hence class II behaviour, in two ways. First they simply separate the metal ions, so they are never less than 5 Å apart (Table 7). This is much too great a distance for any direct overlap between metal orbitals. The second role of the bridging
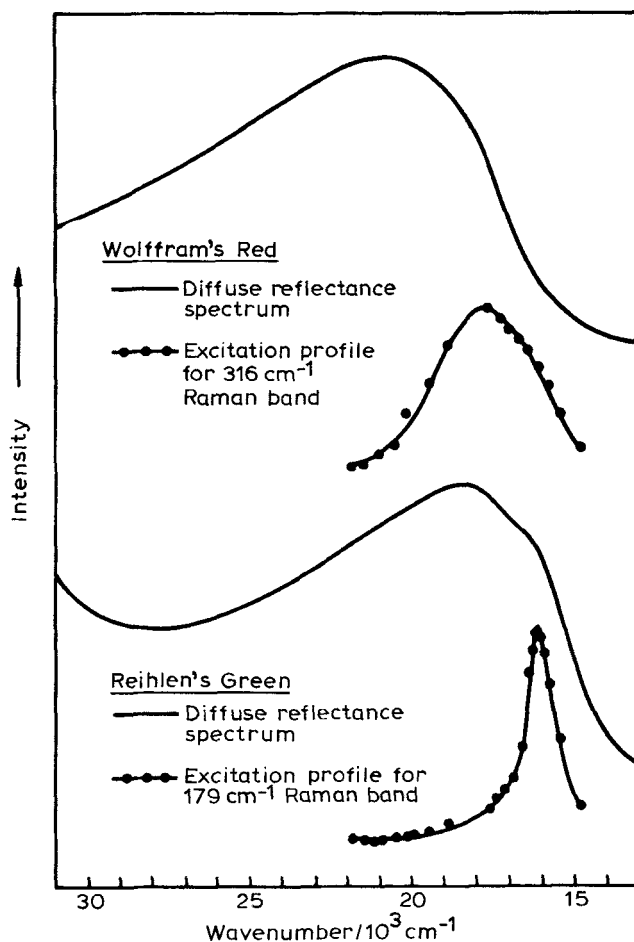
FIG. 21. Resonance Raman enhancement profiles of Wolfram's Red and Reihlen's Green Salts compared with their intervalence band profiles (Clark, 1978).

groups is to introduce the possibility of longitudinal electron-phonon interactions. One may view this question most simply against the background of the Mott–Hubbard model (Hubbard, 1963). If one visualizes a chain of atoms, each having a single unpaired electron, then depending on whether the overlap integral between adjacent orbitals is the dominant factor or, alternatively, the repulsion energy which ensues when one attempts to put two electrons on to the same site, so the ground state wavefunction will either be that of a metal or of a magnetic insulator. There is no room in the simplest version of the Hubbard model for a ground state of the kind actually found in the WRS compounds, namely, a chain containing orbitals which are alternately empty and doubly filled. The only way one could arrive at such a ground state is to include the possibility of trapping the charge fluctuation by relaxing the ligands. This is where the bridging groups come in: remove them and (unless there are differences in the equatorial ligands around the metal sites) the way is open to a metallic ground state.

Still, however, there remains the problem of the one-centre Coulomb repulsion. In a chain containing an integral number of electrons per atom it still costs energy to transfer an electron from one site to another, to create the kind of charge fluctuation needed to

get conduction. But if, on average, the number of electrons per site is not integral, the charge fluctuation is built in already, and the only energy required to get conduction is the energy required to move the fluctuation along the chain. Thus the recipe for metallic conduction in a one-dimensional compound is to have no bridging ligands but directly interacting metal ions, and to ensure that there is a genuinely non-integral number of valence electrons per atom. This is precisely what is found in practice.

Following the first work on the structure and physical properties of the prototype one-dimensional metallic conductor $K_2Pt(CN)_4Br_{0.30}3H_2O$ (KCP) in the later 1960s (Krogmann and Hausen, 1968; Krogmann, 1969) a very large number of similar compounds have now been prepared and examined. Some reviews on the class of material are listed among the general references at the end of the present review, but it is certainly worth remarking at this point on the extraordinary upsurge of interest in this field among both chemists and physicists. In part this stems from what may, in the end, turn out to be a chimera, namely the realization in practical terms of Little's (1964) recipe for an excitonic (and hence high temperature) superconductor.

Little's model has been subjected to searching theoretical scrutiny over the last 17 years, but has not been found logically wanting. It calls for an electronically conducting chain, at right angles to which are placed groups of polarizable material, for example conjugated organic ligands. Excitons within these side-chains then couple with the electrons moving along the chain (*see* chapters by Little, and Gutefreund and Little, in Keller, 1977, for a recent description of the model). A second reason for the physicists' interest in the KCP salts is that many years ago Peierls (1955), in a very simple and elegant theorem, demonstrated that one-dimensional metallic conductors ought to be inherently unstable to distortions which would open a gap in the electron density-of-states at the Fermi surface, thus rendering them semiconductors. In a word, purely one-dimensional metallic conductors ought not to exist! Here, we shall do no more than review very briefly the evidence about the KCP series, emphasizing the role played by mixed-valency.

A feature common to all compounds of the KCP type is a chain of closely spaced metal atoms formed by stacking square-planar ML_4 complexes, were M is Ni, Pd or Pt and L a ligand such as CN^-, oxalate, diphenylglyoximate or a planar macrocycle like phthalocyanine. Mixed valency is achieved by partially oxidizing the metal ions to an average oxidation state $(II + x)$, x being usually about 0.3. Partial oxidation is accomplished in two ways. Counter-ions, both cations and anions, occupy channels between the stacks of planar complex ions, often accompanied by water molecules which create a hydrogen-bonded framework and hence link the one-dimensional metallic chains. Mixed valency in the metal chains comes about either by introducing extra anions (as, for example, on going from $K_2Pt(CN)_43H_2O$ to $K_2Pt(CN)_4Cl_{0.32}3H_2O$, Fig. 22) or by removing some of the cations (e.g. in $K_{1.75}Pt(CN)_41.5H_2O$, Fig. 23). Metal complexes of more highly conjugated ligands can be partly oxidized by iodine, which is incorporated in the channels between the metal chains as I_3^- (Gleizes, Marks and Ibers, 1975; Schramm *et al.*, 1980). An example is shown in Fig. 24. If we write a general formula for compounds of this kind as $A_mML_nX_p(H_2O)_q$ Table 9 gives a survey of known examples.

Not surprisingly in view of the fact that the average oxidation state has increased, the metal-metal spacings in the mixed valency compounds are all less than in the parent divalent compounds. Average oxidation states in the KCP series cluster around 2.30, and there is quite a good correlation between this quantity and the Pt–Pt spacing, as shown in Fig. 25.

Whilst in a few of the compounds the metal atoms lie on special points in the unit cell, so that the metal–metal spacings are constrained to be equal, in the majority of the KCP series this is not the case (Stucky, Schultz and Williams, 1977). Nevertheless, in most examples the spacings are almost equal within experimental error (e.g. Fig. 23). No differ-
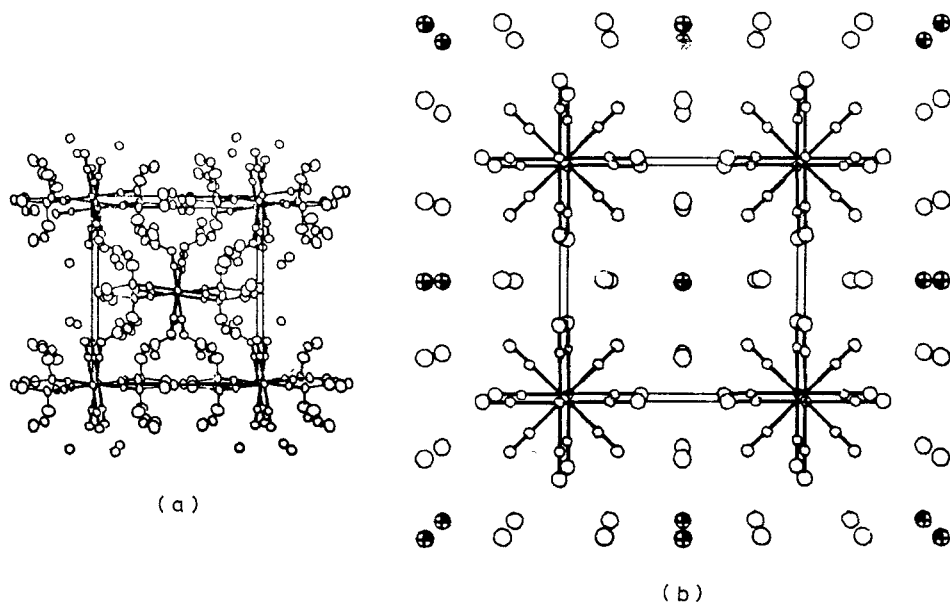
FIG. 22. The crystal structures of (a) $K_2Pt(CN)_43H_2O$, (b) $K_2Pt(CN)_4Cl_{0.32}3H_2O$ (Williams *et al.*, 1974; Washecheck *et al.*, 1976).
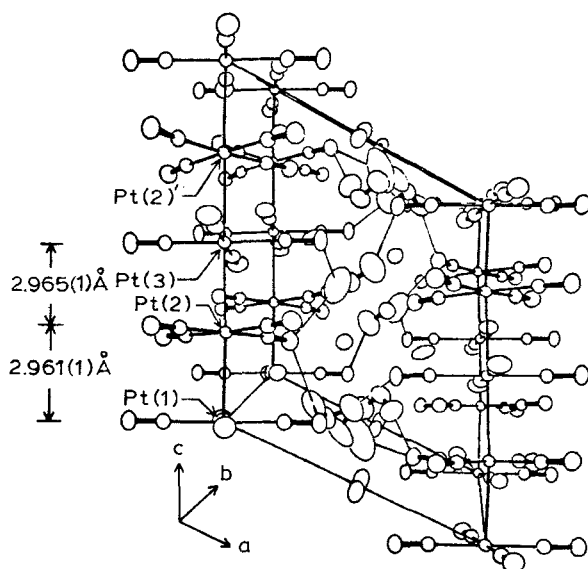
FIG. 23. The crystal structure of $K_{1.75}Pt(CN)_41.5H_2O$ (Keefer *et al.*, 1976).

ences in the Pt–C, or other bond lengths and angles within the complexes have ever been detected so the average oxidation state of the metal is genuinely non-integral and the compounds should be considered as RD class III. Other physical evidence pointing in the same direction includes infrared and Raman spectroscopy (Rousseau *et al.*, 1974) showing only one type of Pt–C and C–N modes, Mössbauer spectroscopy (Ruegg, Kuse and Zeller, 1973) showing only a single broad [195]Pt line, and [195]Pt NMR, which has a Knight

FIG. 24. The crystal structure of $Ni(dpg)_2(I_3)_{0.33}$ (Gleizes *et al.*, 1975).

TABLE 9. The formulae of conducting metal chain compounds $A_mML_nX_p(H_2O)_q$ (Reis and Petersen, 1978; Underhill and Watkins, 1980)
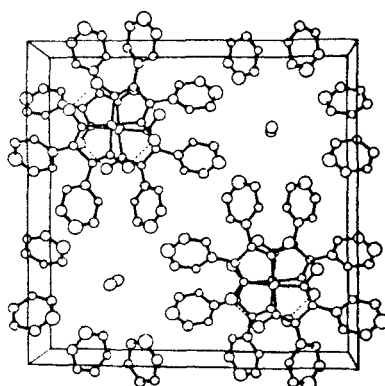
(1) Anion non-stoichiometry

(a) M = Pt, L = CN, n = 4

A:	K	K	NH_4	Rb	Rb	Cs	Cs	$C(NH_2)_3$
X:	$Br_{0.30}$	$Cl_{0.32}$	$Cl_{0.30}$	$Cl_{0.30}$	$(HF_2)_{0.26-0.4}$	$F_{0.19}$	$(N_3)_{0.25}$	$Cl_{0.25}$
q:	3	3	3	3	0–1.67	0		1

(b) A = O, M = Ni, L = planar macrocycle, X = I_3, q = 0

L:	OMTBP	TBP	PC	DPG	OMTBP
p:	0.35	0.33	0.33	0.33	0.97

(2) Cation non-stoichiometry

(a) M = Pt, L = CN, X = —

A:	K	Rb	Cs
m:	1.75	1.73	1.72
q:	1.5	x	x

(b) M = Pt, L = oxalate, X = —

A:	K	Rb	Co	Mg
m:	1.6	1.67	0.83	0.82
q:	1.2	1.5	6	6
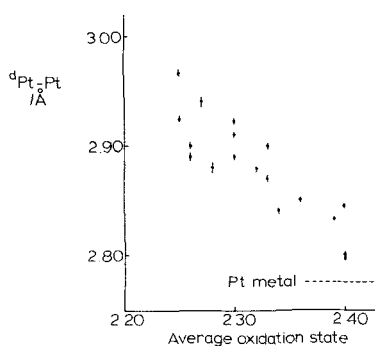
FIG. 25. Variation of Pt–Pt spacing in KCP analogues with average oxidation state.

Mixed valency chemistry
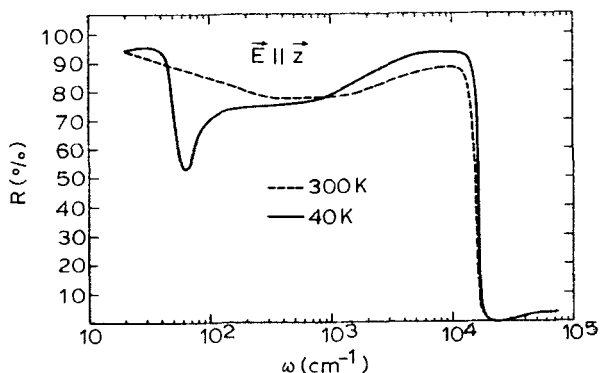
FIG. 26. Reflectivity of KCP with E//z from the far infrared to the ultraviolet (Bruesch *et al.*, 1975).

shift relative to the divalent precursor salts, but again only a single line (Niedoba *et al.*, 1973). Finally, the XPS shows all the Pt atoms in KCP are equivalent (Butler, Rousseau and Buchanan, 1973).

Like the WRS compounds, the optical properties of the KCP salts are extremely anisotropic, and it has even been suggested that they could be used as infrared polarizers. With the incident electric vector parallel to the chains they have a high reflectivity from the far infrared up to 15 000 cm^{-1}, giving the crystals a copper-bronze colour (Fig. 26).

FIG. 27. Specific conductivity of KCP parallel and perpendicular to the metal chain axis as a function of temperature (Zeller and Beck, 1974).

Using Eqs. (43)–(45), but with $\omega_g = 0$ because we are dealing with a metal, the reflectivity has been analysed to give the plasma frequency $\omega_p \sim 2.0$ eV, $\varepsilon_1(\infty) = 2.1$ and τ, the electron relaxation time, is 3.2×10^{-15} seconds (Wagner et al., 1973; Bruesch, Strassler and Zeller, 1975). These figur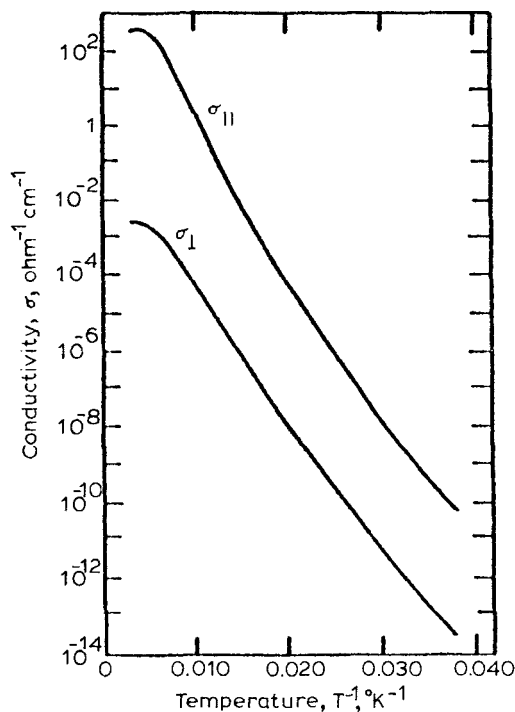es should be compared with those in Table 8. Complications occur at low frequencies, where modes arising from the instability of the one-dimensional metal envisaged by Peierls (1955) come into play. We will not discuss these here, but refer the reader to other reviews (e.g. Keller, 1975, 1977).

As expected for class III mixed valency compounds both the KCP and partly oxidized Ni macrocyclic compounds have high electrical conductivities at room temperature, which are also markedly anisotropic (Fig. 27). In the KCP salts the conductivity falls with decreasing temperature, indicating that at low temperature there is, indeed, a gap in the electron density-of-states as required by Peierls' theorem. The $NiLI_x$ compounds, on the other hand, become more conducting at low temperatures though in one instance there is evidence for a sharp metal-insulator transition.

In this brief account we have not been able to do justice to the range and subtlety of the structural and physical experiments on the class III metal chain compounds. Neither have we mentioned any of the other class III mixed valency compounds containing chains, such as $Hg_{2.86}AsF_6$ and $M_xPt_3O_4$ whose properties (including, in the former case, super-conductivity) are under intensive investigation. For recent accounts, see Hatfield (1979).

CONCLUSION

This review has tried to bring together some of the very disparate strands in contemporary mixed valency chemistry. In doing so many aspects have been ignored, or mentioned only briefly in passing. For example, mixed valency plays an important part in the colouring of minerals and rocks, and is now widely studied by mineralogists (e.g. Burns, 1970; Smith and Strens, 1976). Examples of mixed valency have even been found in moon rocks! (Loeffler, Burns and Tossell, 1975). Other fields which I have scarcely mentioned here, but which have proved a fruitful source of mixed valency materials, are the biological metal clusters such as the ferredoxins and the purely inorganic clusters found in many 'metal rich' phases, e.g. Nb_6Cl_{14} and $M_xMo_6S_8$, the latter of exceptional interest because they are superconductors with relatively high T_c (up to 14 K) and the highest critical fields presently known (Odermott et al., 1974). Nevertheless, the static and vibronic models described provide a useful framework for understanding many of the physical properties of mixed valency compounds though some questions, particularly on the application of the quantitative models to extended lattice compounds, remain to be answered. It can be predicted quite confidently that there will be ample new material for another review of this topic in 10 years' time.

REFERENCES

Reviews on aspects of mixed valency chemistry and physics.

BROWN, D. B. (ed.) (1980). *Mixed Valence Compounds: Theory and Applications in Chemistry, Physics, Geology and Biology*, D. Reidel Publishing Co. Articles on many aspects of mixed valency.

COWAN, D. O., LEVANDA, C., PARK, J. and KAUFMAN, F. (1973). *Acc. Chem. Res.*, *6*, 1. Mixed valency ferrocene chemistry.

HATFIELD, W. E. (ed.) (1979). *Molecular Metals*, Plenum Press. Contains many reviews of conducting chain compounds.

HOLM, R. H. (1977). *Acc. Chem. Res.*, *10*, 427. Mixed-valency iron-sulphur clusters related to ferredoxins.

KELLER, H. J. (ed.) (1975). *Low-dimensional Cooperative Phenomena*, Plenum Press. Contains several reviews about one-dimensional mixed valency compounds.

KELLER, H. J. (ed.) (1977). *Chemistry and Physics of One-dimensional Metals*, Plenum Press.

MILLER, J. S. and EPSTEIN, A. J. (1976). *Prog. Inorg. Chem.*, *20*, 1. One-dimensional complexes.

MILLER, J. S. and EPSTEIN, A. J. (eds.) (1978). *Ann. N.Y. Acad. Sci.*, *313*. Many articles on mixed-valency dimers and chains.

SMITH, G. and STRENS, R. G. J. (1976). *The Physics and Chemistry of Minerals and Rocks*, Wiley. Mixed valency absorption in minerals.

UNDERHILL, A. E. and WATKINS, D. M. (1980). *Chem. Soc. Rev.*, *9*, 429. One-dimensional class III mixed-valency compounds.

WONG, E. Y. and SCHATZ, P. N. (1981). *Prog. Inorg. Chem.*, *28*. Review of the PKS vibronic model of mixed valency.

ALLEN, G. C. and HUSH, N. S. (1967). *Prog. Inorg. Chem.*, *8*, 357.

ANEX, B. G. and SIMPSON, W. T. (1960). *Rev. Mod. Phys.*, *32*, 466.

ATKINSON, L. and DAY, P. (1969). *J. Chem. Soc.*, *A*, 2423.

BARROWCLIFFE, T., BEATTIE, I. R., DAY, P. and LIVINGSTONE, K. (1967). *J. Chem. Soc. A*, 1810.

BEATTIE, J. K., HUSH, N. S. and TAYLOR, P. R. (1976). *Inorg. Chem.*, *15*, 992.

BEATTIE, J. K., HUSH, N. S., TAYLOR, P. R., RASTON, C. L. and WHITE, A. H. (1977). *J. Chem. Soc.*, *Dalton Trans.*, 1121.

BREER, H., ENDRES, H., KELLER, H. J. and MARTIN, R. (1978). *Acta Cryst.*, *B34*, 2295.

BROWN, D. B., ROBIN, M. B., MCINTYRE, J. D. E. and PECK, W. E. (1970). *Inorg. Chem.*, *9*, 2315.

BROWN, K. L. and HALL, D. (1976). *Acta Cryst.*, *B32*, 279.

BRUESCH, P., STRASSLER, S. and ZELLER, H. R. (1975). *Phys. Rev.*, *B12*, 219.

BUNKER, B. C., DRAGO, R. S., HENDRICKSON, D. N., RICHMAN, R. M. and KESSEL, S. L. (1978). *J. Amer. Chem. Soc.*, *100*, 3805.

BURKE, G., LATSCHA, H. P. and PRITZKOW, H. (1976). *Z. Naturforsch.*, *31b*, 1285.

BURNS, R. G. (1970). *Mineralogical Applications of Crystal Field Theory*, Cambridge University Press.

BURROUGHS, P., HAMNETT, A., MCGILP, J. F and ORCHARD, A. F. (1975). *J. Chem. Soc.*, *Faraday Trans. II*, *71*, 177.

BURROUGHS, P., HAMNETT, A. and ORCHARD, A. F. (1974). *J. Chem. Soc.*, *Dalton Trans.*, 565.

BUTLER, M. A., ROUSSEAU, D. L. and BUCHANAN, D. N. E. (1973). *Phys. Rev.*, *B7*, 61.

CAMPAGNA, M., BUCHER, E., WERTHEIM, G. K., and LONGINOTTI, L. D. (1974). *Phys. Rev. Lett.*, *33*, 165.

CANNON, R. D. (1977). *Chem. Phys. Lett.*, *49*, 299.

CHAZALVIEL, J. N., CAMPAGNA, M., WERTHEIM, G. K. and SHANKS, H. R. (1977). *Phys. Rev.*, *B16*, 697.

CHE, M., FOURNIER, M. and LAUNAY, J. P. (1979). *J. Chem. Phys.*, *71*, 1954.

CIECHANOWICZ, M., GRIFFITH, W. P., PARSON, D., SKAPSKI, A. C. and CLEARE, M. J. (1971). *Chem. Commun.*, 876.

CITRIN, P. H. (1973). *J. Amer. Chem. Soc.*, *95*, 6472.

CITRIN, P. H. and GINSBERG, A. P. (1981). *J. Amer. Chem. Soc.*, (in press).

CLARK, R. J. H., FRANKS, M. L. and TRUMBLE, W. R. (1976). *Chem. Phys. Lett.*, *41*, 287.

CLARK, R. J. H. (1977). *Ann. N.Y. Acad. Sci.*, *313*, 672.

CLARK, R. J. H. (1980). In: *Mixed Valency Compounds*, (Ed. by D. B. Brown), p. 271. D. Reidel: Dordrecht.

COOPER, S. R. and CALVIN, M. (1977). *J. Amer. Chem. Soc.*, *99*, 6623.

CRABTREE, A. N. (1972). Chemistry Part II Thesis, Oxford (unpublished).

CRAVEN, B. M. and HALL, D. (1961). *Acta Cryst.*, *14*, 475.

CREUTZ, C. and TAUBE, H. (1969). *J. Amer. Chem. Soc.*, *91*, 3988.

CREUTZ, C. and TAUBE, H. (1973). *J. Amer. Chem. Soc.*, *95*, 1086.

CREUTZ, C., GOOD, M. L. and CHANDRA, S. (1973). *Inorg. Nucl. Chem. Lett.*, *9*, 171.

CULPIN, D., DAY, P., EDWARDS, P. R. and WILLIAMS, R. J. P. (1965). *Chem. Commun.*, 450. idem. (1968), *J. Chem. Soc. A*, *1*, 838.

DAY, P. (1963). *Inorg. Chem.*, *2*, 452.

DAY, P. (1970). *Endeavour*, *29*, 45.

DAY, P. (1974). *Extended Interactions Between Transition Metal Ions*, p. 234. *Amer. Chem. Soc. Symp. Ser.*, no. 5.

DAY, P. (1975). *Low-dimensional Cooperative Phenomena* (ed. H. J. Keller), p. 191, Plenum Press: New York.

DAY, P. (1977). *Chemistry and Physics of One-dimensional Metals* (ed. H. K. Keller), p. 197. Plenum Press: New York.

DAY, P. (1978). *Ann. N.Y. Acad. Sci., 313*, 9.

DAY, P. (1981). *La Recherche, 12*, 304.

DAY, P. (1981). *Comments on Inorg. Chem.* (in press).

DAY, P., ORCHARD, A. F., THOMSON, A. J. and WILLIAMS, R. J. P. (1965). *J. Chem. Phys., 42*, 1973.

DAY, P., HERREN, F., LUDI, A., GUDEL, H. U., HULLIGER, F. and GIVORD, D. (1980). *Helv. Chim. Acta, 63*. 148.

DAY. P., VETTIER, C. and PARISOT, G. (1978). *Inorg. Chem., 17*, 2319.

DENNER, W., SCHULZ, H. and D'AMOUR, H. (1978), *Naturwissenschaften, 65*, 257.

DZIOBKOWSKI, C. T., WROBLESKI, J. T. and BROWN, D. B. (1981). *Inorg. Chem., 20*, 671, 679.

ELSON, C. M., GULENS, J. G., ITZKOVITCH, I. J. and PAGE, J. A. (1970). *Chem. Commun.*, 875.

ENDRES, H., KELLER, H. J., MARTIN, R. and TRAEGER, U. (1979). *Acta Cryst., B35*, 2880.

ENDRES, H., KELLER, H. J., MARTIN, R., GUNG, H. N. and TRAEGER, U. (1979). *Acta Cryst., B35*, 1885.

ENDRES, H., KELLER, H. J., KEPPLER, B., MARTIN, R., STEIGER, W. and TRAEGER, U. (1980). *Acta Cryst., B35*, 760.

ENDRES, H., KELLER, H. J., MARTIN, R., TRAEGER, U. and NOVOTNY, M. (1980). *Acta. Cryst., B36*, 35.

FELIX, F. and LUDI, A. (1978). *Inorg. Chem., 17*, 1782.

FISCHER, H., TOM, G. M. and TAUBE, H. (1976). *J. Amer. Chem. Soc., 98*, 5512.

FRIEDEL, J. (1969). *Comments on Sol. State Phys., 2*, 21.

FULTON, R. L. and GOUTERMAN, M. (1861). *J. Chem. Phys., 35*, 1059.

GLAUSER, R., HAUSER, U., HERREN, F., LUDI, A., RODER, P., SCHMIDT, E., SIEGENTHALER, H. and WENK, F. (1973). *J. Amer. Chem. Soc., 95*, 8457.

GLEIZES, A., MARKS, T. J. and IBERS, J. A. (1975). *J. Amer. Chem. Soc., 97*, 3545.

HALL, D. and WILLIAMS, P. P. (1959). *Acta Cryst., 11*, 624.

HOFMANN, K. A. and HOSCHELE, K. (1916). *Ber. dt. Chem. Ges., 48*, 20.

HUANG, K. and RHYS, A. (1951). *Proc. Roy. Soc. A, 204*, 413.

HUBBARD, J. (1963). *Proc. Roy Soc. A, 276*, 238.

HUSH, N. S. (1961). *Trans. Faraday Soc., 57*, 557.

HUSH, N. S. (1967). *Prog. Inorg. Chem., 8*, 391.

HUSH, N. S. (1975). *Chem. Phys., 10*, 361.

HUSH, N. S. (1980). In: *Mixed Valence Compounds*, (ed. D. B. Brown), p. 151. Dordrecht: D. Reidel.

HUSH, N. S., EDGAR, A. and BEATTIE, J. K. (1980). *Chem. Phys. Lett., 69*, 128.

INTERRANTE, L. V., BROWALL, K. W. and BUNDY, F. B. (1974). *Inorg. Chem., 13*, 1158.

JØRGENSEN, C. K. (1970). *Prog. Inorg. Chem., 12*, 101.

KEEFER, K. D., WASHECHECK, D. M., ENRIGHT, N. P. and WILLIAMS, J. M. (1976). *J. Amer. Chem. Soc., 98*, 233.

KELLER, R., FENNER, J. and HOLZAPFEL, W. B. (1974). *Mat. Res. Bull., 9*, 1363.

KIRKWOOD, J. G. and WESTHEIMER, F. H. (1938). *J. Chem. Phys., 6*, 509.

KRENTZIEN, H. and TAUBE, H. (1976). *J. Amer. Chem. Soc., 98*, 6379.

KROGMANN, K. and HAUSEN, H. D. (1968). *Z. anorg. Chem., 358*, 67.

KROGMANN, K. (1969). *Angew. Chem. Int. Ed., 8*, 35.

LAWTON, S. L. and JACOBSON, R. A. (1966). *Inorg. Chem., 5*, 743.

LEVANDA, C., BECHGAARD, K. and COWAN, D. O. (1976). *J. Org. Chem., 41*, 2700.

LEVANDA, C., BECHGAARD, K., COWAN, D. O., MUELLER-WESTERHOFF, U. T., EILBRACHT, P., CANDELA, G. A. and COLLINS, R. A. (1976). *J. Amer. Chem. Soc., 98*, 3181.

LEVICH, V. G. (1970). *Physical Chemistry, an Advanced Treatise* (ed. H. Eyring, D. Hendrickson and W. Jost), vol. 9B. New York: Academic Press.

LITTLE, W. A. (1964). *Phys. Rev., 134*, A1416.

LOEFFLER, B. M., BURNS, R. G. and TOSSELL, J. A. (1975). *Proc. 6th Lunar Sci. Conf.*, p. 2663.

LUDI, A. (1980). In: *Mixed Valence Compounds*, (ed. D. B. Brown), p. 25. Dordrecht: D. Reidel.

MAGNUSON, R. H. and TAUBE, H. (1972). *J. Amer. Chem. Soc.*, *94*, 7213.

MARCUS, R. A. (1956). *J. Chem. Phys.*, *24*, 966.

MARCUS, R. A. (1965). *J. Chem. Phys.*, *43*, 679.

MARKHAM, J. J. (1959). *Rev. Mod. Phys.*, *31*, 956.

MARTIN, D. S. (1971). *Inorg. Chim. Acta Rev.*, *5*, 107.

MATSUMOTO, N., YAMASHITA, M. and KIDA, S. (1978). *Bull. Chem. Soc. Japan*, *51*, 3514.

MAYOH, B. and DAY, P. (1972). *J. Amer. Chem. Soc.*, *94*, 2885.

MAYOH, B. and DAY, P. (1973). *J. Chem. Soc., Dalton Trans.*, 846.

MAYOH, B. and DAY, P. (1974). *Inorg. Chem.*, *13*, 2273.

MEYER, T. J. (1978). *Ann. N.Y. Acad. Sci.*, *313*, 496.

MEYER, T. J. (1979). *Chem. Phys. Lett.*, *64*, 417.

MINGARDI, M. and SIEBRAND, W. (1975). *J. Chem. Phys.*, *62*, 1074.

MORRISON, W. H. and HENDRICKSON, D. N. (1973). *J. Chem. Phys.*, *59*, 380.

MORRISON, W. H., KROGSUND, S. and HENDRICKSON, D. N. (1973). *Inorg. Chem.*, *12*, 1998.

MUELLER-WESTERHOFF, U. T. and EILBRACHT, P. (1972). *J. Amer. Chem. Soc.*, *94*, 9272.

NIEDOBA, H., LANNOIS, H., BRINKMANN, D., BRUGGER, R. and ZELLER, H. R. (1973). *Phys. Stat. Sol.*, (b) *58*, 309.

ODERMATT, R., FISCHER, O., JONES, H. and BONGI, G. (1974). *J. Phys.*, *C7*, L13.

ORCHARD, A. F. and THORNTON, G. (1977). *J. Chem. Soc., Dalton Trans.*, 1238.

PAPPAVASSILIOU, G. C., LAYEK, D. and THEOPHANIDES, T. (1980). *J. Raman Spect.*, *9*, 69.

PAPPAVASSILIOU, G. C. and ZDETSIS, A. D. (1980). *J. Chem. Soc., Faraday Trans.*, *II*, *76*, 104.

PARASKEVAIDIS, C. E. and PAPATRIANTAFILLOU, C. (1980). *Chem. Phys.*, *45*, 393.

PEIERLS, R. E. (1955). *Quantum Theory of Solids*, p. 108, Oxford University Press.

PIEPHO, S. B., KRAUSZ, E. R. and SCHATZ, P. N. (1978). *J. Amer. Chem. Soc.*, *100*, 2996.

PLAKSIN, P. M., STONFER, R. C., MATHEW, M. and PALENIK, G. J. (1972). *J. Amer. Chem. Soc.*, *94*, 2121.

POWERS, M. J., CALLAHAN, R. W., SALMON, D. J. and MAYER, T. J. (1976). *Inorg. Chem.*, *15*, 894.

POWERS, M. J., CALLAHAN, R. W., SALMON, D. J. and MEYER, T. J. (1976). *Inorg. Chem.*, *15*, 1457.

POWERS, M. J., SALMON, D. J., CALLAHAN, R. W. and MEYER, T. J. (1976). *J. Amer. Chem. Soc.*, *98*, 6731.

POWERS, M. J. and MEYER, T. J. (1978). *J. Amer. Chem. Soc.*, *100*, 4393.

PRASSIDES, K. (1980). Chemistry Part II Thesis, Oxford (unpublished).

RICHARDSON, D. (1981). PhD. Thesis, Stanford University, California.

RIEDER, K. and TAUBE, H. (1977). *J. Amer. Chem. Soc.*, *99*, 789.

ROBIN, M. B. and DAY, P. (1967). *Adv. Inorg. Chem. and Radiochem.*, *10*, 247.

ROUSSEAU, D. L., BUTLER, M. A., GUGGENHEIM, H. J., WEISMAN, R. B. and BLOCH, A. N. (1974). *Phys. Rev.*, *B10*, 2281.

RUEGG, W., KUSE, D. and ZELLER, H. R. (1973). *Phys. Rev.*, *B8*, 952.

RYAN, T. D. and RUNDLE, R. E. (1961). *J. Amer. Chem. Soc.*, *83*, 2814.

SCHATZ, P. N., PIEPHO, S. B. and KRAUSZ, E. R. (1978). *Chem. Phys. Lett.*, *55*, 539.

SCHRAMM, C. J., SCARINGE, R. P., STOJAKOVIC, D. R., HOFMANN, B. M., IBERS, J. A. and MARKS, T. J. (1980). *J. Amer. Chem. Soc.*, *102*, 6702.

STEVENS, K. W. H. (1953). *Prog. Roy. Soc.*, *A219*, 542.

STREKAS, T. C. and SPIRO, T. G. (1976). *Inorg. Chem.*, *15*, 974.

STUCKY, G. D., SCHULTZ, A. J. and WILLIAMS, J. M. (1977). *Ann. Rev. Mat. Sci.*, *7*, 301.

STYNES, H. C. and IBERS, J. A. (1971). *Inorg. Chem.*, *10*, 2304.

SULLIVAN, B. P. and MEYER, T. J. (1980). *Inorg. Chem.*, *19*, 321.

TAUBE, H. (1978). *Ann. N.Y. Acad. Sci.*, *313*, 481.

THIELE, G. (1977). Quoted by Clark, R. J. H., *Ann. N.Y. Acad. Sci.*, *313*, 672.

THOMAS, T. W. and UNDERHILL, A. E. (1969). *Chem. Commun.*, 725.

THOMAS, T. W. and UNDERHILL, A. E. (1971). *J. Chem. Soc. A*, 512.

TOM, G. M., CREUTZ, C. and TAUBE, H. (1974). *J. Amer. Chem. Soc.*, *96*, 7827.

TOM, G. and TAUBE, H. (1975). *J. Amer. Chem. Soc.*, *97*, 5310.

TRICKER, M. J., ADAMS, I. and THOMAS, J. M. (1972). *Inorg. Nucl. Chem. Lett.*, *8*, 633.

VERWEY, E. J. W., HAAYMAN, P. J., ROMEIJN, F. C. and VAN OOSTERHOUT, G. W. (1950). *Philips Res. Report*, *5*, 173.

WAGNER, H., GESERICH, H. P., BALTZ, R. V. and KROGMANN, K. (1973). *Sol. State Commun.*, *13*, 659.

WALLEN, J., BROSSET, C. and VANNERBERG, N. G. (1962). *Arkiv. Kem.*, *A18*, 541.

WALTON, E. G., CORVAN, P. J., BROWN, D. B. and DAY, P. (1976). *Inorg. Chem.*, *15*, 1737.

WASHECHECK, D. M., PETERSEN, S. W., REIS, A. H. and WILLIAMS, J. M. (1976). *Inorg. Chem.*, *15*, 74.

WERNER, A. (1896). *Z. anorg. Chem.*, *12*, 46.

WILLIAMS, J. M., PETERSON, J. L., GERDES, H. M. and PETERSEN, S. W. (1974). *Phys. Rev. Lett.*, *33*, 1079.

WONG. K. Y., SCHATZ, P. N. and PIEPHO, S. B. (1979). *J. Amer. Chem. Soc.*, *101*, 2793.

YAMADA, S. and TSUCHIDA, R. (1956). *Bull Chem. Soc. Japan*, *29*, 894.

YAMASHITA, M., MATSUMOTO, N. and KIDA, S. (1978). *Inorg. Chim. Acta*, *31*, L381.

ZELLER, H. R. and BECK, A. (1974). *J. Phys. Chem. Sol.*, *35*, 77.